Sonographic Anatomy of the Skin, Appendages, and Adjacent Structures

2

Ximena Wortsman, Jacobo Wortsman, Laura Carreño, Claudia Morales, Ivo Sazunic, and Gregor B.E. Jemec

The normal anatomy from a practical approach correlating clinical, ultrasound and histologic images

Contents

X. Wortsman, MD (✉)
Department of Radiology and Dermatology,
Institute for Diagnostic Imaging and Research of the Skin and Soft Tissues, Clinica Servet,
University of Chile, Faculty of Medicine,
Almirante Pastene 150, Providencia, Santiago, Chile
e-mail: xwo@tie.cl, xworts@yahoo.com, www.sonoskin.com

J. Wortsman, MD
Department of Medicine,
Southern Illinois University School of Medicine,
3128 Temple Drive, Springfield, IL 62704, USA

L. Carreño, MD • C. Morales, MD
Department of Pathology, Dermopathology Section,
Hospital Clinico Universidad de Chile, Faculty of Medicine,
University of Chile, Santiago, Chile
e-mail: lcarrenotoro@gmail.com; claudiamohuber@gmail.com

I. Sazunic, MD
Department of Dermatology, Dermatopathology Section,
Faculty of Medicine,
Histodiagnostico Malaga, University of Chile,
Santiago, Chile

G.B.E. Jemec, MD, DMSci
Department of Dermatology, Health Sciences Faculty,
Roskilde Hospital, University of Copenhagen,
Køgevej 7-13, Roskilde 4000, Denmark
e-mail: gbj@regionsjaelland.dk

X. Wortsman, G.B.E. Jemec (eds.), *Dermatologic Ultrasound with Clinical and Histologic Correlations*,
DOI 10.1007/978-1-4614-7184-4_2, © Springer Science+Business Media New York 2013

2.1 Introduction

The skin is the most superficial and largest body organ, and as such easily accessible to sonographic examination. It is however also a complex organ, and in spite of the approachable location, its great histologic and functional complexities present unique problems that must be addressed in ultrasound imaging.

The skin has a range of passive and active functions. While it mainly serves as the body's envelope protecting it against thermal and physical injuries, it is also the site for the photosynthesis of vitamin D_3, an indispensable factor in bone physiology. Furthermore, the skin regulates body temperature (through direct evaporation of water by the sweat glands or through the insulating properties of fatty tissue); and a communication organ as it connects the external and internal environments through a wide assortment of nerve receptors that serve not only to orientate the body in relation to the environment, but also in communication between individuals [1–3]. These many functions can only be fulfilled if the organ contains a broad range of different tissues and cell types.

Skin disorders are generally expressed with highly specific distribution patterns that reflect regional inhomogeneities in blood and nerve supply, immunologic variability in epitopes/antigens expression, and/or differences in immune cells distribution. Occasionally, primary alterations of superficial structures (tendons, ligaments, muscles, lymph nodes, or bony margins) may also simulate skin pathology or, be secondarily involved by primary skin disorders. Therefore the morphology of both the skin and of the adjacent organs must be properly identified when imaging the skin and establishing the differential diagnosis of a skin disease.

2.2 Technical Considerations

Appropriate sonographic examination of the skin requires both specialized equipment and thorough training of the operator. Initially, important data were generated with dedicated skin ultrasound performed at a fixed high frequency using heavy probes. Technological advances in ultrasound technology have however now opened the possibility for more thorough imaging of both the skin and the adjacent structures, providing a comprehensive and detailed image for analysis. It is now possible to use multichannel ultrasound machines fit with tunable (variable) frequency (≥15 MHz), and light-weight probes, making it possible to study the skin as well as the underlying tissues in a single process. Furthermore, the appearance of compact-linear type ("hockey-shaped" or "foot-print" transducers) has meant that more areas can now be studied because of the transducers' better adaptation to the irregular shape of the skin surface. Additional capabilities for sensitive color or power Doppler testing, extended field of view, and 3D reconstruction are also often useful.

The qualifications required of the operator in this field must include skills in both imaging as well as more than a basic knowledge of dermatology. The combined understanding is needed to properly correlate clinical findings with sonographic images. Real-time interpretation of the results allows for the prompt generation of clinical information, critical for consequent decisions on whether to extend the examination to a corporal segment not included in the initial request, thereby providing clinical utility.

Ultrasonography is not associated with adverse effects, and few preparations are needed in patients. Sedation is however routinely recommended for imaging studies in children younger than 4 years old to prevent movement artifacts as a result of crying or anxiety, as this may affect the spectral representation of the blood flow. Color Doppler ultrasound examination demands an environment that is quiet and comfortable for the child, the parents/guardians, and the operator. After the informed consent is signed by the parents or guardians, chloral hydrate (50 mg/kg) is administered orally; excellent sedation is regularly obtained and the examination is performed approximately 30 min later. The child is monitored with the Modified Aldrete Score (i.e., evaluation of activity, respiration, circulation [blood pressure], consciousness, and oxygen saturation), and discharge is recommended when the score reaches a value of 9 or higher.

To facilitate ultrasound wave focusing to the most superficial skin layers, copious amounts of gel must be applied; preferably, the gel is pre-warmed to decrease patient discomfort. The use of stand-off pads for further focus adjustment is not only unnecessary, but not recommended because the devices may compress small superficial vessels and interfere with the actual imaging process [4]; likewise, intravenous contrast medium is rarely if ever needed for basic studies.

2.3 Sonography of Cutaneous Layers

Like all epithelia, skin integrates passive and active barrier functions, mechanical functions, and other functions in a layered structure. The histologic skin layers such as the epidermis, dermis, and subcutaneous tissue can also be separated into sonographic equivalents of an outer layer (corresponding to the epidermis), a middle layer (dermis), and a deeper layer (subcutaneous tissue, subcutis, or hypodermis) [3, 5] (Fig. 2.1). Although the general organization of the skin is spatially maintained throughout the body, recognition of regional variations is of paramount importance for the correct analysis of sonographic findings.

Significant regional quantitative differences occur. The stratum corneum (i.e., the outermost layer of the epidermis) is thick in the palms and soles, and very thin on the eyelids. The epidermis is generally thinner in the forearm and thicker

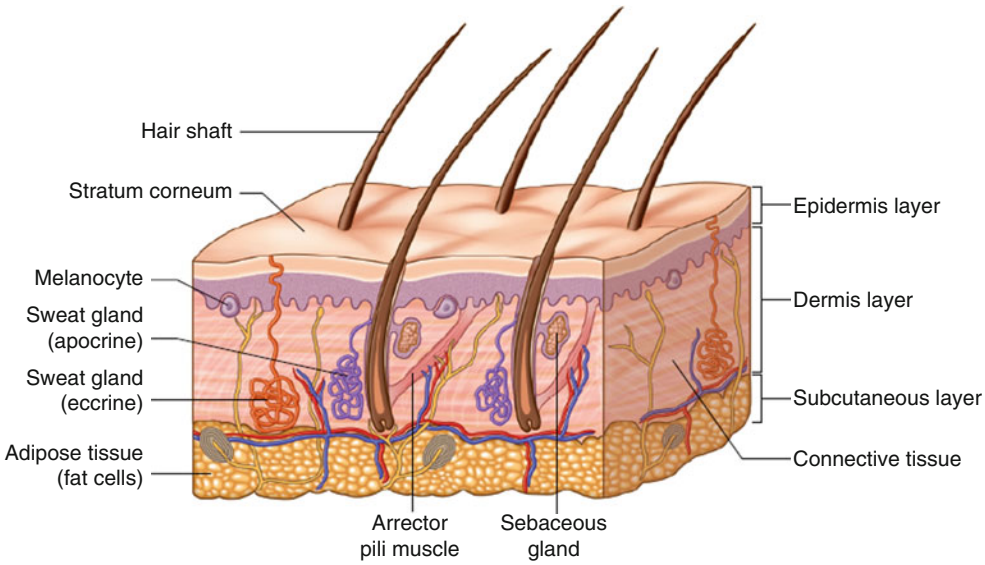

Fig. 2.1 Skin anatomy. Drawing shows the different components of the cutaneous layers

in the plantar or palmar regions; the dermis is thinner in the ventral forearm but thicker in the dorsal region; and the subcutaneous tissue is thinner in the dorsal aspect of the fingers but thicker in the trunk [6].

Qualitative differences also occur. The appendages are obviously also not evenly distributed over the body. Thus, hair follicles are prominent in the scalp, but absent in the soles of the feet (i.e., glabrous skin or devoid of hair). In addition, the skin exhibits important variations in the local density of melanocytes and blood supply [5].

All these characteristic properties must be considered when describing morphology, depth, and structural involvements by cutaneous lesions, as well as reference standards for the different skin imaging modalities.

2.3.1 Epidermis

2.3.1.1 Anatomy

The epidermis has a highly pleiotropic cellular content and is nonvascular. It is nourished through diffusional flow by the dermal circulation. The main cell populations of the epidermis are keratinocytes, melanocytes, and Langerhans cells. Small numbers of other cells, including Merkel cells (associated with sensory functions) are also present. The epidermis is in contiguity with the appendages, specialized dermal structures that transit through the epidermis lined with epithelial cells, with important potential for division and differentiation. Epidermal appendages include the hair follicles, nails, and sweat glands (with its apocrine, eccrine, and apoeccrine variants) and often stretch through the dermis as well, therefore, these will therefore be discussed elsewhere. The pilosebaceous unit is an epidermal invagination that contains the hair follicle (shaft and bulb portions), sebaceous glands, and the erector pili muscle (smooth muscle).

The interfollicular epidermis is divided into four epidermal layers or strata (from the most superficial to the deepest): corneum (acellular layer, keratin, and lipids), granulosum (granular cells), spinosum (prickly cells), and basale or germinativum (basal cells). There is an undulating basement membrane at the junction between epidermis and dermis providing adhesive support and is divided into lamina lucida and lamina densa. The thin lamina lucida lies directly beneath the basal keratinocytes epidermal layer, while the thicker lamina densa is in direct contact with the underlying dermis. These structures are the target of immunologic injury in autoimmune bullous disorders such as bullous pemphigoid and abnormalities in genetic structural disorders such as epidermolysis bullosa.

The epidermal diffusional flow through the dermoepidermal junction is critical for both nutrition supply and metabolite removal (including vitamin D_3). The epidermal appendages are separated from blood vessels, nerves, and cells in their dermal portion by a connective tissue sheath [3, 7].

2.3.1.2 Sonography

Echogenicity is determined by the capability to reflect the sound waves by the predominant or reflective component of the structure being studied; for example, epidermal keratin is highly echogenic, and heavily keratinized areas such as the thicker glabrous skin (palms of the hands and the soles of the feet) appear as bilaminar hyperechoic structures. In the lesser keratinized non-glabrous skin the epidermis appears as only a single, hyperechoic line that offers no major detail for interpretation (Figs. 2.2, 2.3, and 2.4) [4].

2.3.2 Dermis

2.3.2.1 Anatomy

The dermis is a supporting structure histologically dominated by organized bundles of collagen deposited by local fibroblasts providing not only the stroma for the epithelium but also the predominant mechanical functions of the skin.

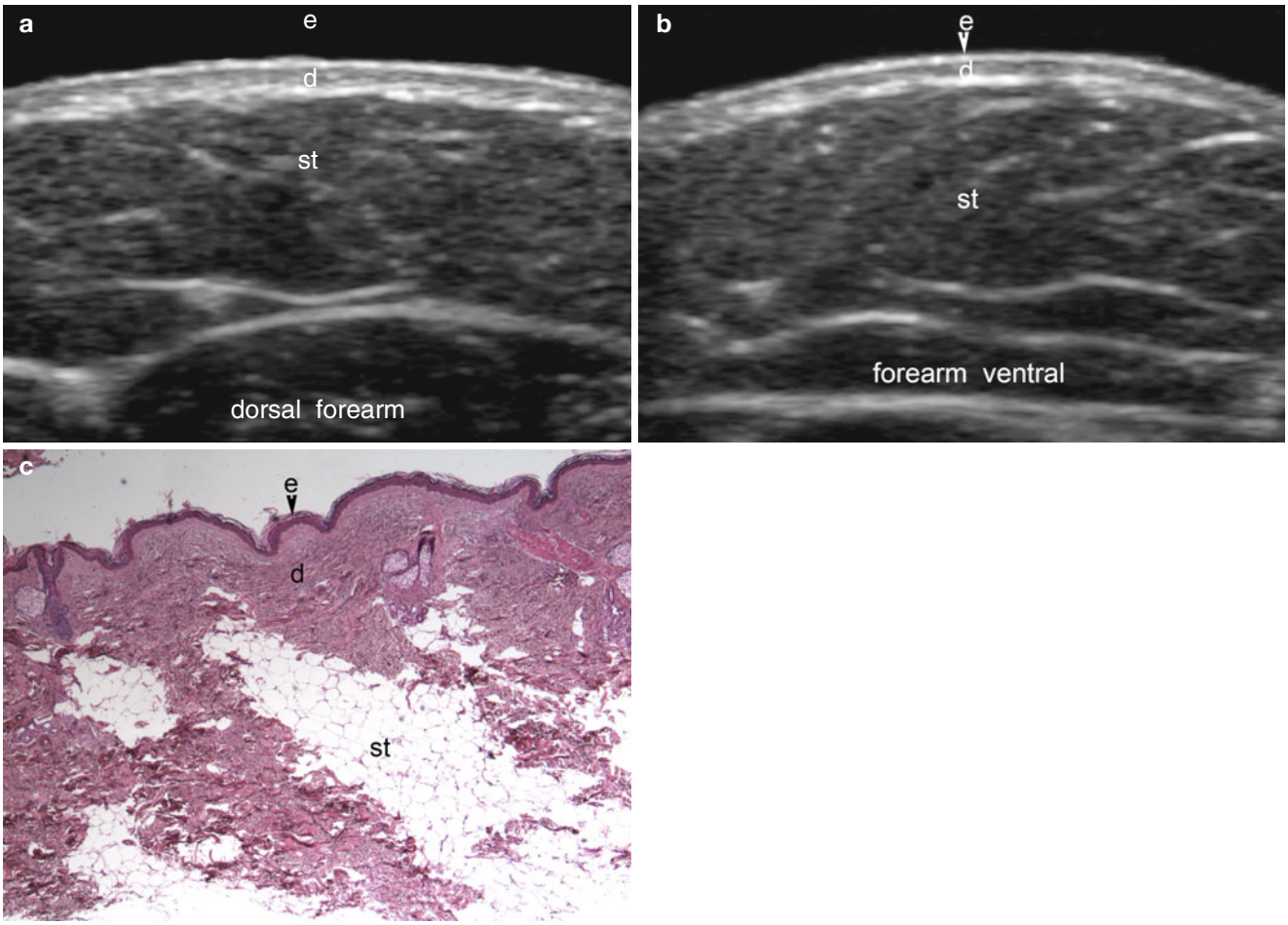

Fig. 2.2 (**a**–**c**) Normal skin, forearm. (**a**, **b**) Ultrasound (transverse view). (**a**) Dorsal forearm and (**b**) Ventral forearm. Note the thin ventral forearm dermis. (**c**) Histology (H&E ×40 zoom) demonstrates thin epidermis and dermis. *Abbreviations*: *e* epidermis, *d* dermis, *st* subcutaneous tissue

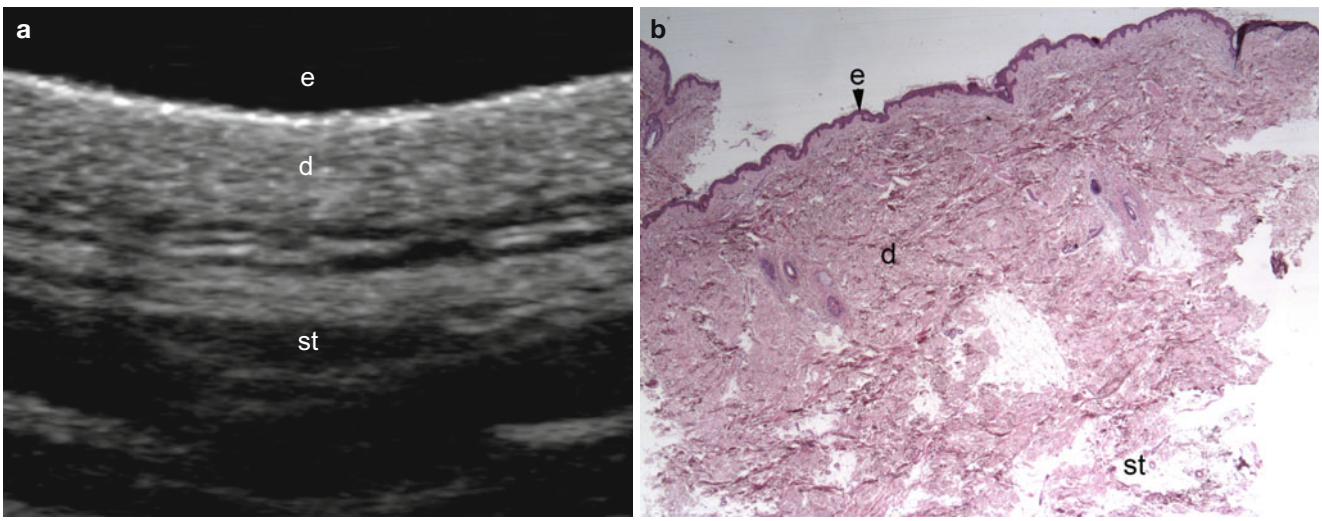

Fig. 2.3 (**a**, **b**) Normal dorsal skin. (**a**) Ultrasound (transverse view). Note the difference in dermis thickness compared to Fig. 2.2. (**b**) Histology (H&E ×40 zoom). Note high dermal collagen density and thickness. *Abbreviations*: *e* epidermis, *d* dermis, *st* subcutaneous tissue

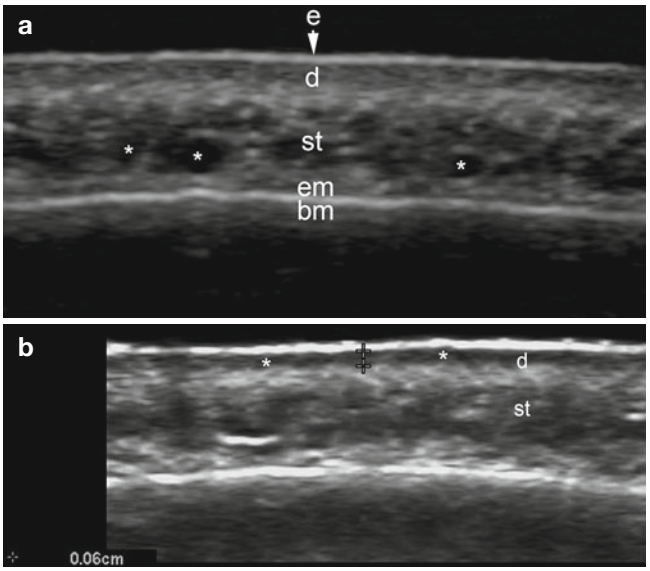

Fig. 2.4 (**a**, **b**) Normal frontal skin. (**a**) Ultrasound (transverse view). Note prominent subcutaneous veins (*). (**b**) Note subepidermal low echogenicity band (*, between markers), a sonographic sign of photoaging. *Abbreviations*: *e* epidermis, *d* dermis, *st* subcutaneous tissue, *em* epicranius muscle, *bm* bony margin of the skull

The dermis content also includes blood vessels, lymphatic vessels, nerve fibers, and the deep portions of hair follicles and sweat glands.

The dermis or corium consists of connective tissue (cells, collagen, and elastic fibers) arranged into two layers: a more superficial papillary dermis and the deeper reticular dermis. The thin papillary dermis is made of loose connective tissue containing mostly capillaries and fibers (elastic and reticular, with sparse collagen content). In the thick reticular dermis the connective tissue is denser, traversed by larger blood vessels, elastic fibers, coarse bundles of collagen fibers arranged in layers parallel to the skin surface, cells (fibroblasts, mast cells), nerve endings, lymphatic vessels, and epidermal appendages. The predominant form of collagen in the dermis is type I, followed by collagen III; the small amount of elastic fibers present in the dermis play an important functional role in the resistance to deformational forces, preventing the sagging of the skin. All dermal components are bound together by a gel-like ground substance made of various glycosaminoglycans (primarily hyaluronic acid, but also chondroitin sulfate), and glycoproteins.

The dermis exhibits a complex vascular system: the papillary dermis is supplied by a superficial vascular plexus at the border between papillary and reticular dermis through a candelabra-like capillary system; other specialized dermal vascular formations include arterio-venous anastomoses and the glomus bodies. Arterio-venous anastomoses function as valves allowing blood to bypass upper dermal capillaries, whereas glomus bodies, found in the fingertips, are rich vascular plexus of capillaries and lymphatics vessels that run along the dermal papillae, perpendicular to the skin surface. The dermal lymphatic circulation runs through an extensive network loosely arranged into superficial and deep plexuses [3, 8].

2.3.2.2 Sonography

Dermal echogenicity is determined by the collagen component that produces a hyperechoic band but trophic changes, as seen in older individuals after chronic exposure to sunlight, change dermal echogenicity from a single homogenous reflection to a more complex pattern with an additional subepidermal hypoechoic band (SLEB). The pathologic substrate for the latter is elastosis, a combination of elastin degeneration and local glycosaminoglycans deposition [4, 9] (Figs. 2.2, 2.3, and 2.4). With the current equipment, rarely blood flow is detected in the normal dermis on color Doppler.

2.3.3 Subcutaneous Tissue-Subcutis-Hypodermis

2.3.3.1 Anatomy

The subcutaneous fat is a tissue compartment further divided into lobules containing adipose cells and separated by thin fibro-vascular septa. The septa consist of collagen and reticulin fibers, and house blood, lymphatic vessels and cutaneous nerves. Each lobule is supplied by a small muscular artery (250–500 μm diameter) branching from the septa into centrilobular arterioles (100–300 μm in diameter) that generate capillary networks around each individual adipocyte; postcapillary venules drain into larger peripheral veins that also run along the septa. This arrangement has important clinical connotations because interferences with the arterial supply result in diffuse intra-lobular changes (panniculitis, mostly lobular), whereas venous occlusive disorders manifest with septal and paraseptal alterations (panniculitis, mostly septal). Of note, and in contrast to the rich connections of dermal vessels, the blood supply of the adipose microlobule is terminal, implying that there are no capillary connections between adjacent microlobules or between dermis and subcutaneous fat. As far as lymphatic circulation is concerned, subcutaneous fat septa contain dense lymphatic plexuses that transverse into the subcutaneous tissue, at first parallel to the surface of the skin and then perpendicular, to penetrate the deep fascia and drain into regional lymph nodes [10–12].

2.3.3.2 Sonography

The subcutaneous tissue with its fatty lobules appears hypoechoic with interspersed hyperechoic fibrous septa. Subcutaneous circulation can be visualized with color

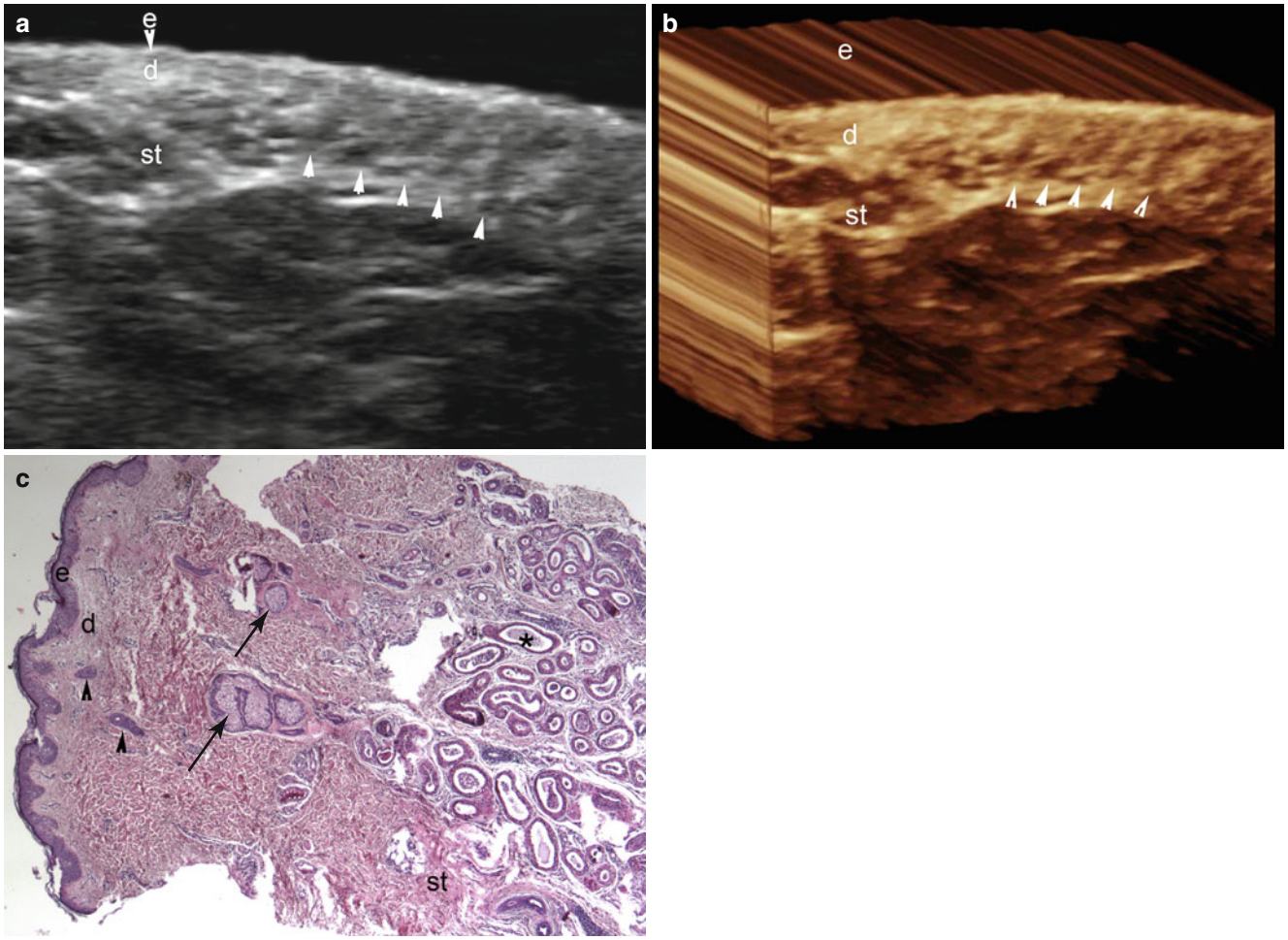

Fig. 2.5 (**a**–**c**) Normal skin at the axillary region. (**a**) Ultrasound (transverse view). The prominent dermal hypoechoic bands in the oblique axis correspond to hair follicles (*arrowheads*). (**b**) 3D ultrasound (transverse view). (**c**) Histology (H&E ×40 zoom) showing hair follicles (*arrowheads*) and sebaceous glands (*arrows*) in the dermis and apocrine glandular tissue (*) in the subcutaneous layer

Doppler examination that normally shows a low-flow pattern, detectable in arterial and venous vessels of the subcutaneous tissue [4] (Figs. 2.2, 2.3, 2.4, 2.5, and 2.6).

2.4 Appendages

2.4.1 Nail

2.4.1.1 Anatomy

The nail unit has a complex structure that involves three separate areas: the ungual plate that consists mostly of keratin, the nail bed that includes the matrix region, and the periungual region that includes the proximal and lateral nail folds. The nail plate presents keratinized epithelial cells and shows a curved shape (longitudinal and transverse axes) that facilitates attachment in the lateral and proximal nail folds. It is composed of dorsal and ventral layers that run transversely and a central layer that runs in longitudinal axis that may favor the resistance of the nail to trauma. The nail bed mostly presents a thin epidermis with prominent longitudinal ridges and a dermal layer without sebaceous or follicular appendages. The ungual matrix is the germinal layer that provides the keratinized cells that compose the nail plate. It is located in the proximal nail underlying the lunula (half moon) and also presents lateral proximal extensions (also called wings that are closely attached to the distal part of the lateral ligaments of the distal interphalangeal joint). The dermis underlying the ungual matrix shows prominent collagen. The periungual folds (lateral and proximal) are the cutaneous sites of insertion of the nail plate. Vascular supply to the nail is performed by four digital arteries, two on each side of the finger (ventral and dorsal aspect). The ventral (palmar) branches provide the main supply to the fingers and they show anastomoses in the distal arcades (dorsal and ventral). The ventral arch is located in the maximal padding of the finger pulp and the dorsal arch lies distal to the distal interphalangeal joint providing supply for the nail fold, extensor

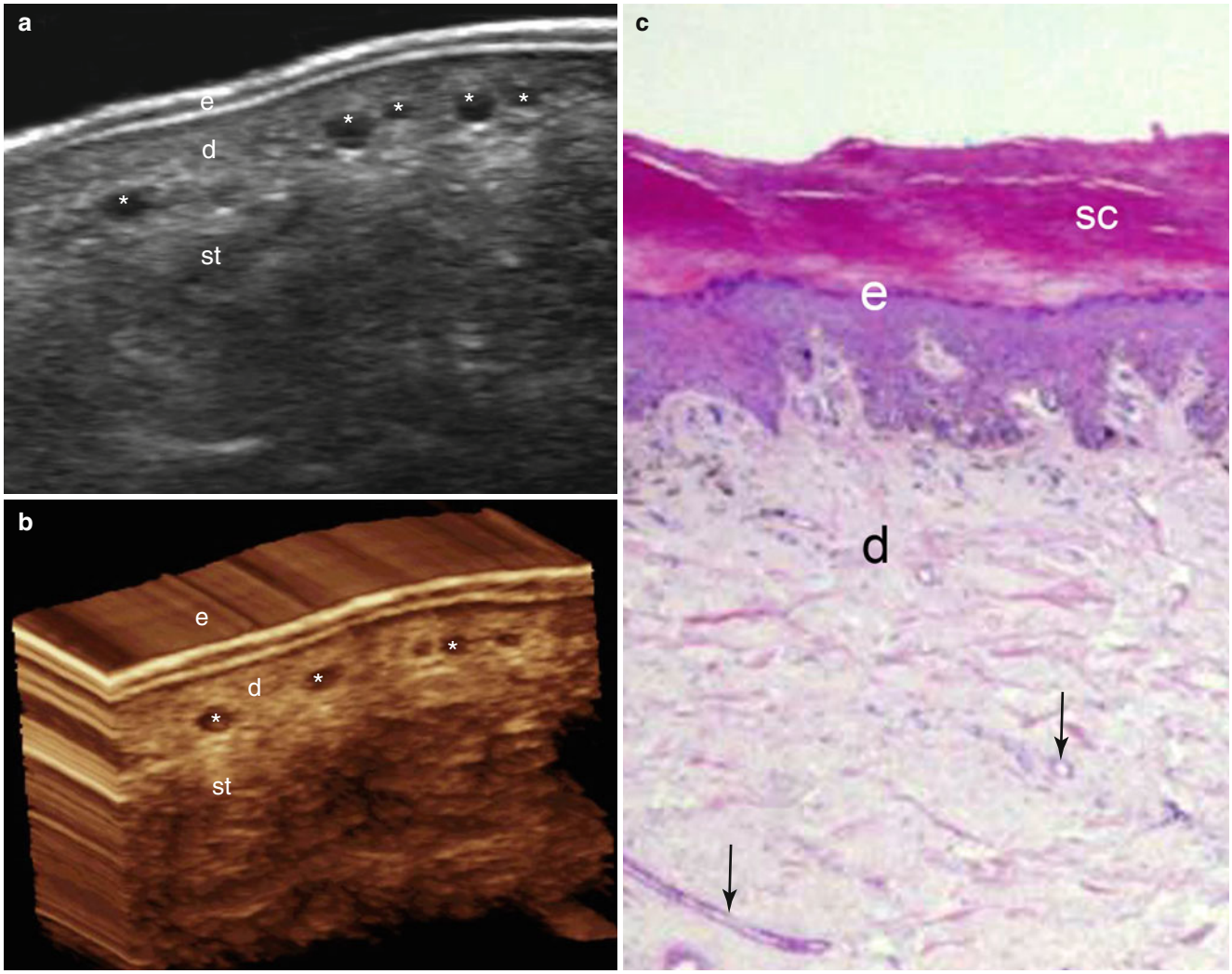

Fig. 2.6 (**a**–**c**) Normal plantar skin. (**a**) Ultrasound (transverse view) shows a bilaminar hyperechoic pattern of the epidermis. Dermal venous vessels (*) are prominent. (**b**) 3D ultrasound. (**c**) Histology (H&E ×40 zoom) showing marked stratum corneum (*sc*) thickness of the plantar epidermis, some thin vessels (*arrows*) and lack of hair follicles. *Abbreviations*: *e* epidermis, *d* dermis, *st* subcutaneous tissue, *sc* stratum corneum

tendon insertion, and the nail matrix. Deep and superficial veins conform a prominent network in the dorsal and ventral regions. Glomus bodies that are clusters of arteriovenous shunts surrounded by a prominent myoneural component are also present in the nail bed. It is supposed that these glomus bodies can serve in the regulation of the capillary network and may support the preservation of the peripheral blood flow under extreme cold conditions [13].

2.4.1.2 Sonography

The different parts of the nail apparatus have characteristic sonographic profiles. The ungual plate appears as a hyperechoic bilaminar structure: the two parallel lines, called dorsal and ventral plate, separated by an almost virtual hypoechoic space that tends to disappear at very high sound frequencies (≥22 MHz). The nail bed appears hypoechoic, but may turn slightly hyperechoic at proximal levels, beneath the ungual matrix. The periungual skin (lateral and proximal nail folds) has the sonographic morphology of normal skin with corresponding cutaneous layers, except for the almost total absence of adipose tissue. However, fatty lobules can be discerned in the hyponychium (distal periungual tissue) and the distal palmar aspect of the fingers. A pattern of low-flow vascularity (arterial and venous) is frequently detected in the nail bed close to the hyperechoic bony margin of the distal phalanx [14] (Figs. 2.7 and 2.8).

2.4.2 Hair

2.4.2.1 Anatomy

Hair, a unique mammalian trait, has important functional roles in thermoregulation, physical protection, sensory activity, and social interactions. Histologically, hair is divided

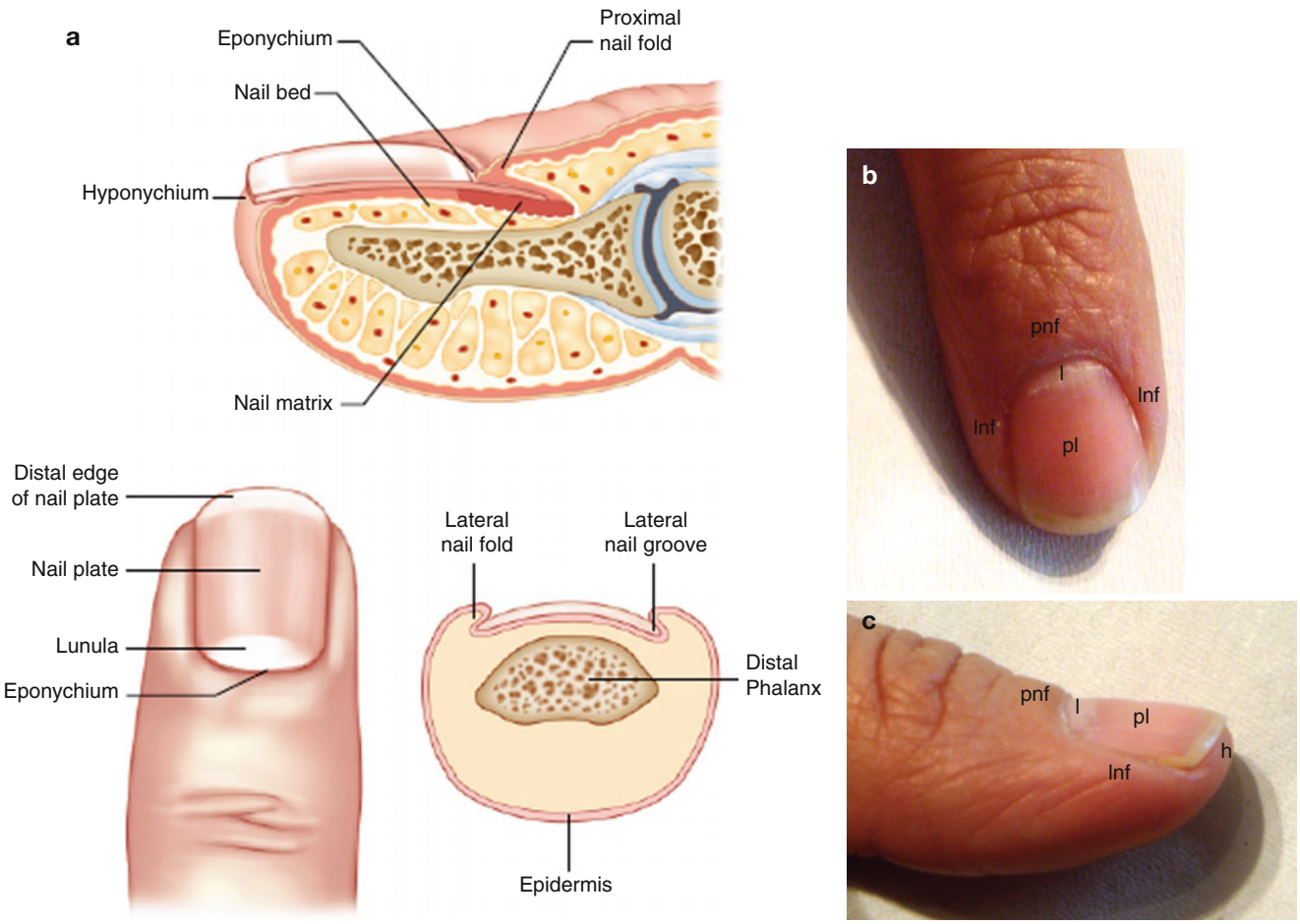

Fig. 2.7 (**a**–**c**) Nail anatomy. (**a**) Schematic representation of the nail. (**b**) Clinical frontal view of the nail. (**c**) Clinical lateral view of the nail. *Abbreviations*: *pl* ungual plate, *l* lunula, *pnf* proximal nail fold. *lnf* lateral nail fold, *h* hyponychium

into the hair follicle, located in the dermis, and the hair tract or shaft that emerges to the skin surface. Hair tracts are made of terminally differentiated keratinocytes produced by the hair follicles and consist of an outer layer or cuticle, analogous to the stratum corneum of the epidermis; a middle layer or cortex, made of hard keratin; and, an inner layer or medulla made of soft keratin. Hair follicles are distributed over the entire surface of the body with the notable exceptions of the soles of the feet, palms of the hands, glans penis, clitoris, labia minora, and muco-cutaneous junctions. The complex of sebaceous glands and hair follicle, in combination with the pili erector muscle form the pilosebaceous unit. At the proximal end or base of the hair follicle is the hair bulb, lying deep within the dermis and reaching down to the subcutaneous fat in the face. Because the hair bulb harbors a population of stem cells, the rich facial population of hair follicles results in rapid re-epithelization, even after deep cutaneous wounds. Contraction of the pili erector that connects the deep portion of the follicle to the superficial dermis (under control by the sympathetic nervous system) causes the follicle to assume a vertical direction ("goosebumps"). Hair density is highest in the scalp, where it is supplied by a centripetal vascular network derived from branches of the internal and external carotid arteries; the blood vessels traverse the subcutaneous tissue from the circumference of the scalp toward the midline, while progressively decreasing in size. After birth hair reaches maturity, undergoing active growth when hair follicles become anchored in the subcutaneous tissue, to be lost and regenerated periodically through cycles of growth (anagen), apoptosis-driven regression (catagen), and quiescence (telogen). Hair follicle orientation is oblique to the skin surface in Caucasians, and almost parallel in individuals of African ancestry; whereas in people of Asian ancestry, hair follicles are oriented vertically producing straight hairs [7, 8, 14–16].

2.4.2.2 Sonography

Hair follicles appear as slightly oblique hypoechoic bands usually wider at the bottom, occupying the dermis but reaching the subcutaneous border at maturity; scalp hair tracts are mostly

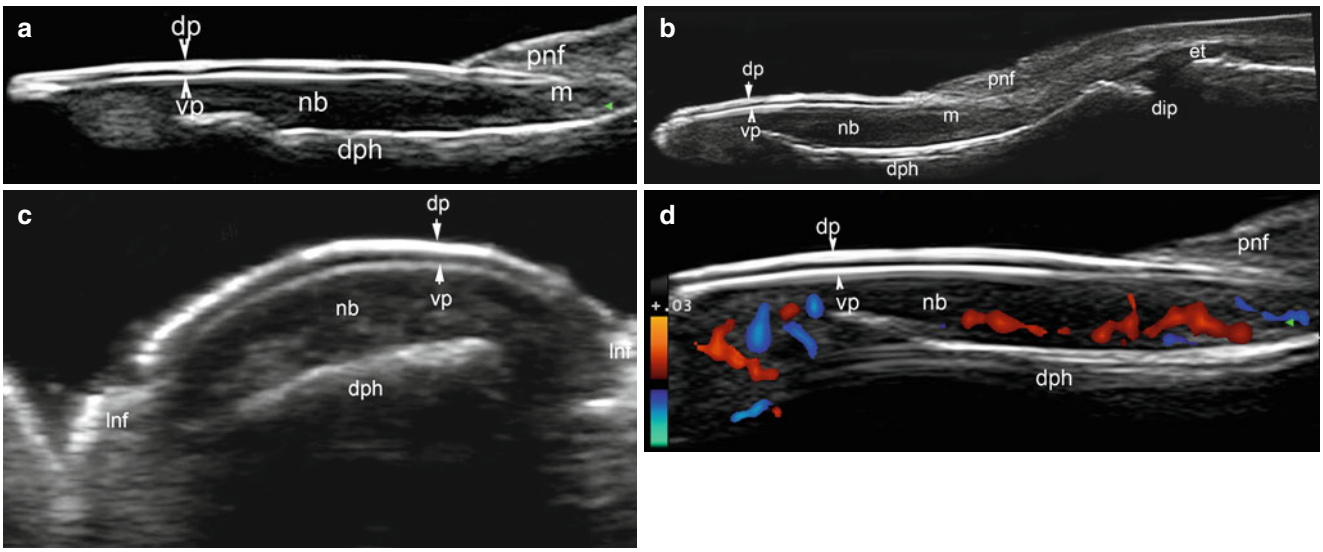

Fig. 2.8 (**a**–**d**) Nail anatomy. (**a**) Ultrasound of the nail unit (longitudinal view). (**b**) Ultrasound of the nail unit (longitudinal extended panoramic view) including the insertion of the extensor tendon (*et*) and the distal interphalangeal joint (*dip*). (**c**) Ultrasound of the nail unit (transverse view). Note lateral nail folds (*lnf*). (**d**) Color Doppler ultrasound (longitudinal view) showing visible blood flow within the nail unit. *Abbreviations*: *nb* nail bed, *dp* dorsal plate, *vp* ventral plate, *pnf* proximal nail fold, *lnf* lateral nail fold, *dph* distal phalanx, *dip* distal interphalangeal joint, et extensor tendon distal insertion

trillaminar hyperechoic structures, with the two outer lines corresponding to the cuticle-cortex complex and the inner line to the medulla. Vellous hairs such as the eyelashes may lack the center (medulla) and appear as a monolayer hyperechoic line.

Ultrasound makes it possible to identify the growth cycle phase, with shallow follicles marking the telogen phase (i.e., hair follicles located in the upper dermis) and deep follicles, the anagen phase(i.e., hair follicles with their bottom part reaching the border between the dermis and the subcutaneous tissue); intermediate stages indicate the catagen phase [17]. The variations in the orientation of the hair follicles (axis) can be recorded at the time of imaging examination to help prevent alopecia post-scalp surgery (Figs. 2.9 and 2.10).

2.4.3 Sebaceous Glands

2.4.3.1 Anatomy

Sebaceous glands are epidermal appendages and form an important part of the pilosebaceous unit. They are holocrine glands (the cellular cytoplasm is the secretion) that are widely distributed throughout the skin but most associated with hair and therefore concentrated in the face and scalp; they are absent from the palm of the hands and soles and dorsum of the feet. Sebaceous glands often open directly into the hair follicle and their secretion is sebum, an oily complex of triglycerides, fatty acids and their breakdown products, wax esters, squalene, and cholesterol and cholesterol esters. Because of its lipid-hydrophobic composition, sebum is a lubricant protecting the skin against friction while making it more impervious to moisture [14]. Meibomian and Montgomery's glands are sebaceous glands without associated hairs.

2.4.3.2 Sonography

Normal sebaceous glands are not visible by sonography on the machines currently in use, except as a part of the pilosebaceous unit.

2.4.4 Eccrine Glands

2.4.4.1 Anatomy

Sweat glands are eccrine glands (secrete a watery fluid) that are also widely distributed, being most concentrated in the palms of the hands, soles of the feet, and axillae; they are absent in the vermillion border of the lips, the external ear canal, the nail beds, the labia minora, the glans penis and the inner aspect of the prepuce. Sweat glands have a dermal coiled secretory portion and a straight distal duct connection to the epidermis. Sweat gland activity is controlled by the thermoregulatory center in the hypothalamus through sympathetic nerves [15]; sweat exerts a cooling effect on the body through heat loss by water evaporation.

2.4.4.2 Sonography

Normal eccrine glands are not visible using current ultrasound equipment.

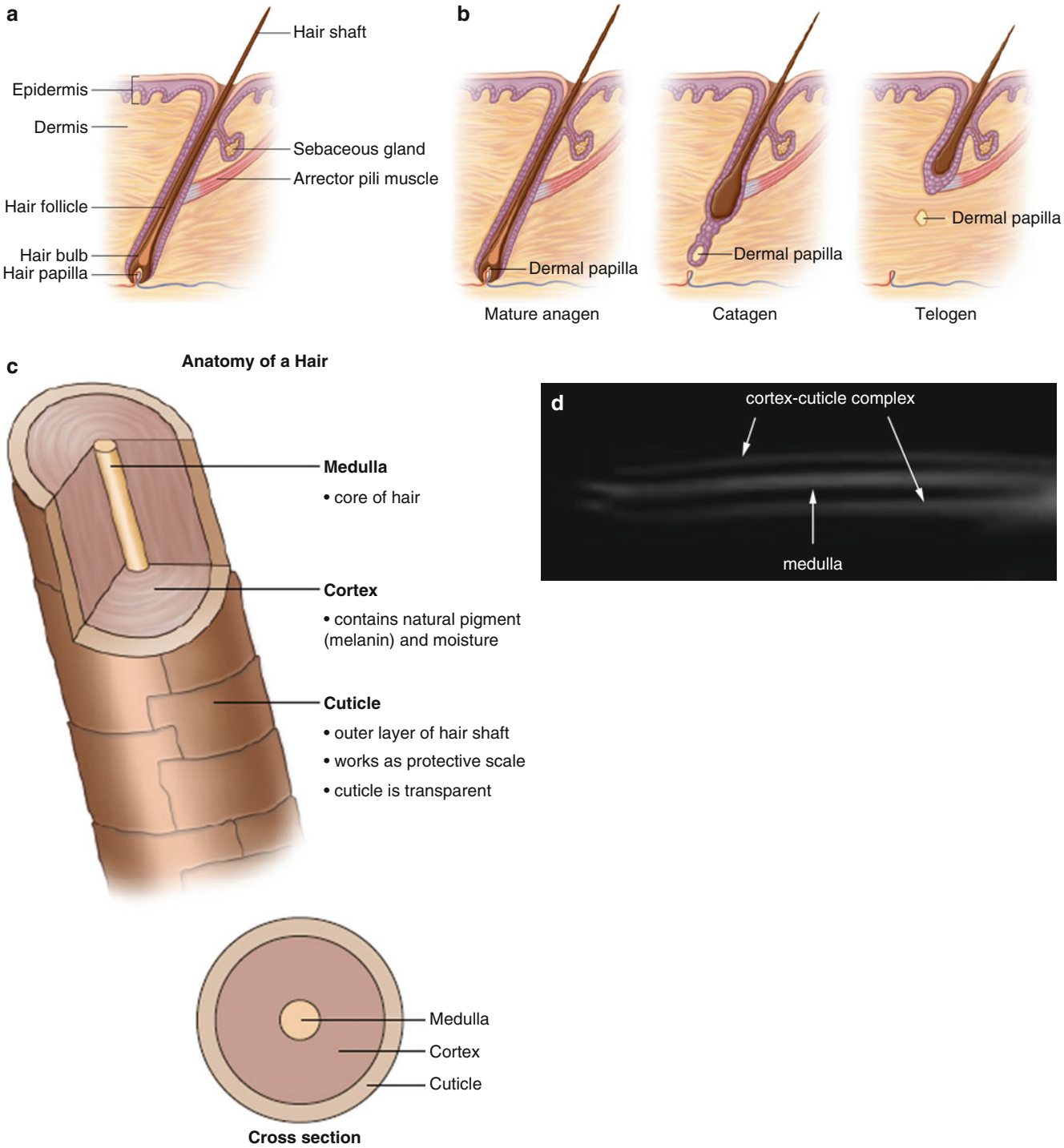

Fig. 2.9 (**a**–**d**) Hair. (**a**) Hair follicle structure. (**b**) Growth cycle of the hair follicle. (**c**) Normal structure of the hair tract. (**d**) Ultrasound of scalp hair shaft.

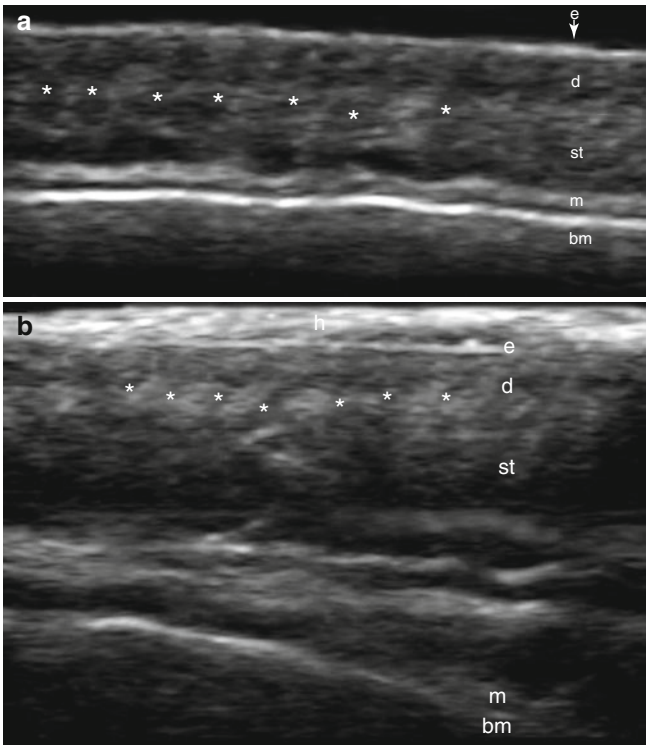

Fig. 2.10 (**a**, **b**) Sonographic anatomy of the scalp (longitudinal views). Note in dermis the hypoechoic, oblique direction of hair follicles (*). (**a**) Frontal region. (**b**) Occipital region. Note increased thickness of subcutaneous tissue. *Abbreviations*: *h* condensed hair tracts, *e* epidermis, *d* dermis, *st* subcutaneous tissue, *m* epicranius muscle, *bm* bony margin of the skull

2.4.5 Apocrine and Mammary Glands

2.4.5.1 Anatomy

Apocrine glands include cellular content in the secretory product and are found in the axillae, anogenital region; modified apocrine glands are found in the external ear canal (represented by the ceruminous glands), the eyelids (Moll's glands), and breasts (mammary glands). Most apocrine glands do not start functioning until after puberty and the secretion is often odorous [3, 8, 15]. Mammary glands are modified glands of the skin located on the milk lines. The glands are thought to be modified apocrine glands, and 15–20 glands are combined into the compound gland recognized clinically as the breast. The breast consists of secretory alveoli, lactiferous ducts, supportive connective tissue, and adipose tissue.

2.4.5.2 Sonography

The apocrine glands are not visible using sonography. Mammary glands are seen as hyperechoic fibroglandular tissue interspersed with hypoechoic fatty lobules. The subcutaneous tissue in the breast region may show a variable thickness of the fat component according to age, which is more prominent during late adulthood. Thin anechoic ducts can be detected in the areola region, and low flow vascularity is usually seen in the normal parenchyma.

2.5 Anatomy and Variants of Structures Adjacent to the Skin

2.5.1 Lymph Nodes

2.5.1.1 Anatomy

The oval-shaped organs belong to the immune system and show an outer capsule, mainly cellular, and an inner medulla with prominent ducts and sinuses. A fibrous macrocapsule surrounds the capsule with the exception of the vascular hilum region. B and T cells, plasma cells, and macrophages as well as a network of lymph sinuses ad ducts are present in the lymph nodes. Palpation of lymph nodes is a part of the routine clinical examination of patients, and the location of major conglomerates of lymph nodes is therefore well known. However, palpation is operator-dependent and additional information is therefore welcome, particularly where aberrant or abnormal nodes are found, or malignancy suspected.

2.5.1.2 Sonography

Lymph nodes appear as oval-shaped structures with hypoechoic rim (cortex) and hyperechoic center (medulla). The cortical rim is usually thin and of uniform thickness in all views. Color Doppler ultrasound shows the usually centrally located vascular hilum, generally detected in one of the aspects and typically consisting of low-flow arterial and venous vessels (Fig. 2.11).

2.5.2 Tendons

2.5.2.1 Anatomy

Tendons are composed of parallel bundles of collagen fibers that are held together by proteoglycans and connective tissue. A synovial sheath (lining) or a paratenon (loose connective tissue) can wrap around the tendon to protect it from friction or trauma. Superficial tendons are rarely directly involved in skin disease, but generalized diseases such as storage diseases and rheumatological diseases may require a more detailed description of tendons and the entheses.

2.5.2.2 Sonography

Tendons are hyperechoic cords, reflecting their high collagen content that exhibit a parallel fibrilar pattern. The normal synovial sheath is usually non-visible to ultrasound, with the exception of large groups of tendons such as the common extensor compartment in the wrist. The normal Achilles or patellar tendons present a "paratenon" usually not detected on ultrasound; synovial sheaths can contain a thin film of anechoic and compressible fluid surrounding the tendon that serves as a lubricant. Importantly, tendons may exhibit the sonographic artifact "anisotropy" (i.e., appearing bright on the screen when the ultrasound beam strikes the tendon at a 90° angle, but dark at other angles of approach). Anisotropy

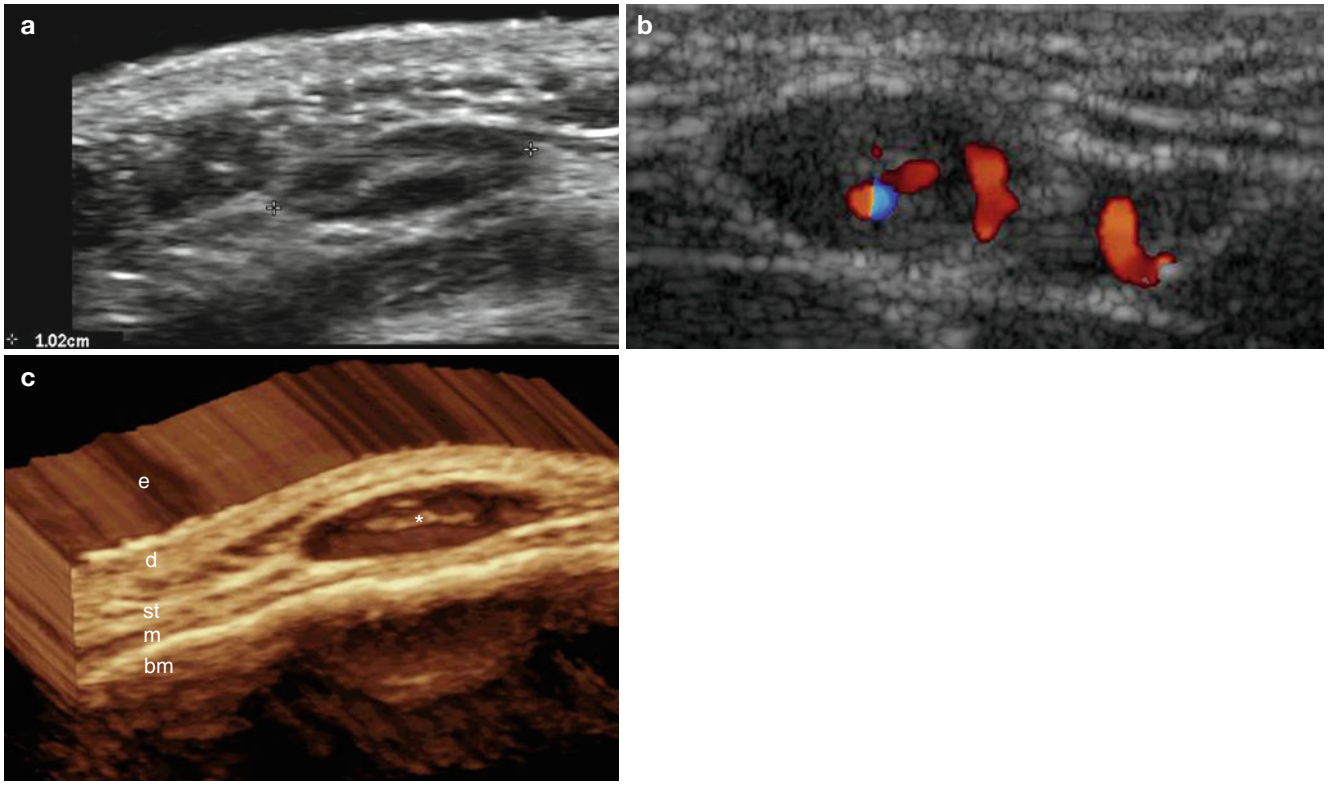

Fig. 2.11 (**a**–**c**) Lymph node anatomy. (**a**) Ultrasound (gray scale) shows 1.02 cm oval-shaped structure (between markers) with continuous hypoechoic cortex and well-defined hyperechoic center. (**b**) Color Doppler ultrasound. Note significant hilar blood flow. (**c**) 3D reconstruction. Note lymph node with the hyperechoic center (*). *Abbreviations*: *e* epidermis, *d* dermis, *st* subcutaneous tissue, *m* muscle, *bm* bony margin

may occasionally become a useful tracking signal in locating tendinous structures and should also be taken into account in the differential diagnosis of the tendon hypoechogenicity typical of tendinous tear or tendinosis. On sonography, accessory tendons exhibit morphology similar to normal tendons and maintain the hyperechoic fibrilar pattern. A common example is the accessory tendon of the abductor pollicis longus in the first extensor compartment of the wrist. Visualization of the accessory variant improves markedly if fluid is present within the synovial sheath of the tendon. Doubtful cases can be assisted using comparisons with the contralateral side. Ultrasound can also provide invaluable assistance by making it possible to visualize tendon movements in real time [18] (Fig. 2.12).

2.5.3 Muscle

2.5.3.1 Anatomy

Muscles are composed of myocytes, formed into muscle fibers are arranged in myofibrils that are packed in sarcomeres containing the proteins (actine and myosine, among others) that are necessary for the contraction process. Sequentially, the muscle fibers are surrounded by connective tissue layers that originate from the endomysium (i.e., covering of a muscle fiber) to the epimysium, covering the entire muscle. Skeletal muscles generally have one middle portion (belly) and two tendons (proximal and distal insertions), belly variations in number or shape result in the unipennate, bipennate, and/or circumpennate configurations. Bellies may also be separated by fibrous intersections, in the rectus abdominus or as a single belly and connect to multiple points of origins as in the quadriceps muscle. Several muscles are in close proximity to the skin in (e.g., the hands where assessment may be needed when inflammation is present). Accessory muscles are additional, anomalous, or supernumerary structures, usually discovered as asymptomatic findings but occasionally may cause soft-tissue swelling, becoming clinically relevant.

2.5.3.2 Sonography

Skeletal muscles are hypoechoic structures made of thick fascicles separated by hyperechoic adipose-fibrous septa (perimysium), and surrounded by an also hyperechoic fascia (Fig. 2.13). Fat deposits between the muscles can be identified, providing clinically useful inter-muscle separation planes. Sonographically, muscles are usually grouped functionally into compartments that change synchronously during a dynamic study (flexion-extension or rest-contraction) [19]. Accessory or supernumerary muscles

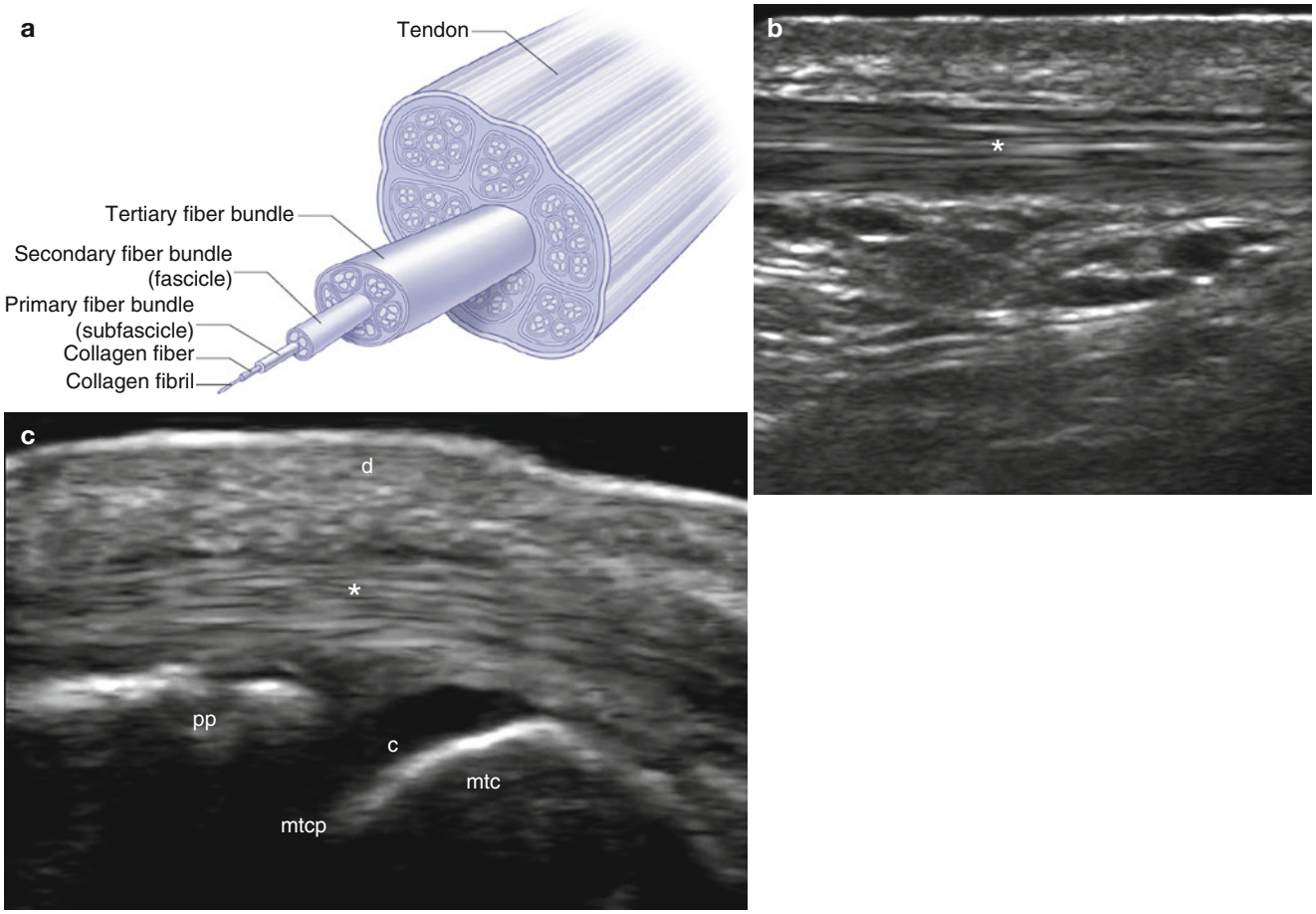

Fig. 2.12 (**a**–**c**) Anatomy of tendons. (**a**) Schematic representation of tendon structure. (**b**) Ultrasound of the anterior tibial tendon (longitudinal view). Note the hyperechoic fibrillar pattern (*). (**c**) Ultrasound of digital flexor tendon (*) at the metacarpophalangeal level in the hand (longitudinal view). *Abbreviations*: *d* dermis, *pp* proximal phalanx, *c* cartilage, *mtc* metacarpal bone, *mtcp* metacarpophalangeal joint

exhibit morphology similar to normal muscles (Fig. 2.14). Dynamic maneuvers may demonstrate the contraction process on short or transverse axis ultrasound, with the muscular belly showing increased anteroposterior size and decreased echogenicity. Common accessory muscles of the upper and lower limbs are listed on Table 2.1. Doubtful cases can be assisted using comparisons with the contralateral side [20].

2.5.4 Cartilage

2.5.4.1 Anatomy

Cartilage is composed of a hydrophilic matrix made of collagen fibers, glycosaminoglycans chondroitin, keratan sulfate, and cells (chondrocytes). According to the proportion of their collagen content, cartilages are classified into fibrocartilage (with high collagen content) and hyaline cartilage (with lower content). Cartilages are devoid of blood vessels and are supplied solely by diffusion from the synovial membrane or bone, and can be involved in locally destructive processes (e.g., Chondrodermatitis helicis of the ear) or systemic autoimmune disease.

2.5.4.2 Sonography

Articular hyaline cartilage appears as a well-defined intensely hypoechoic band adjacent to the hyperechoic bony margin (Fig. 2.15). In contrast, fibrocartilages such as the menisci in the knee or the triangular fibrocartilage in the wrist appear less hypoechoic than the hyaline cartilage with occasional hyperechoic areas reflecting calcium deposits [21].

2.5.5 Bursae

2.5.5.1 Anatomy

Bursae are sac-like structures with viscous fluid content that facilitates the movement of the musculoskeletal structures by reducing friction. Bursae are located superficially in the subcutaneous tissue, as the olecranon bursa in the elbow and the prepatellar bursa in the knee, or have deeper locations such as the subacromiosubdeltoid bursae in the

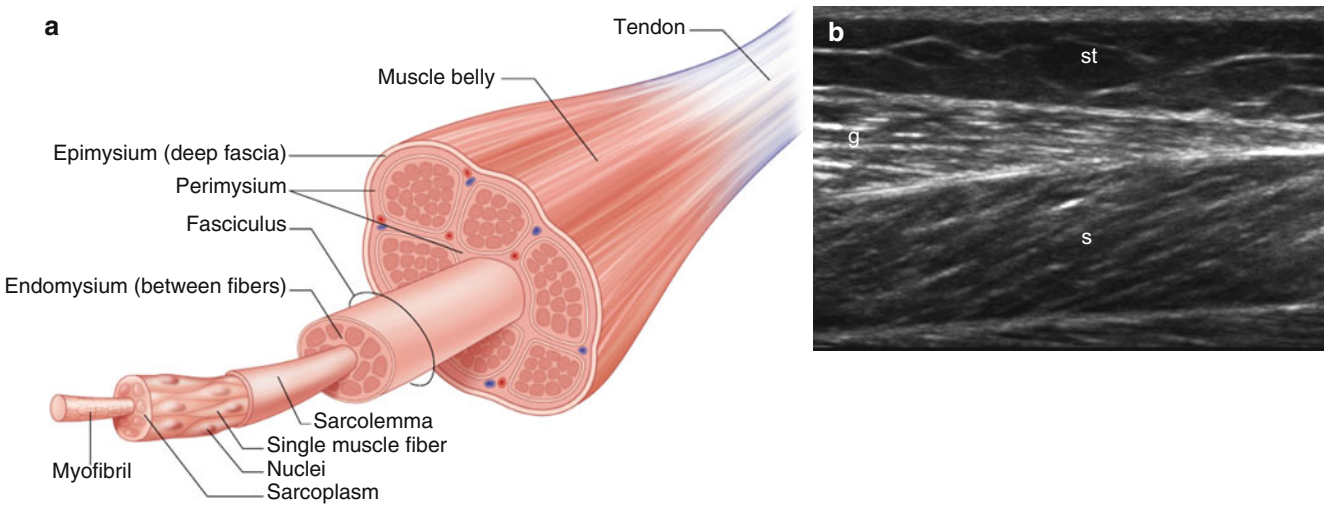

Fig. 2.13 (**a**, **b**) Anatomy of muscle. (**a**) Schematic representation of muscle. (**b**) Ultrasound of calf gastrocnemius muscle (longitudinal view). *Abbreviations*: *st* subcutaneous tissue, *g* gastrocnemius muscle belly, *s* soleous muscle

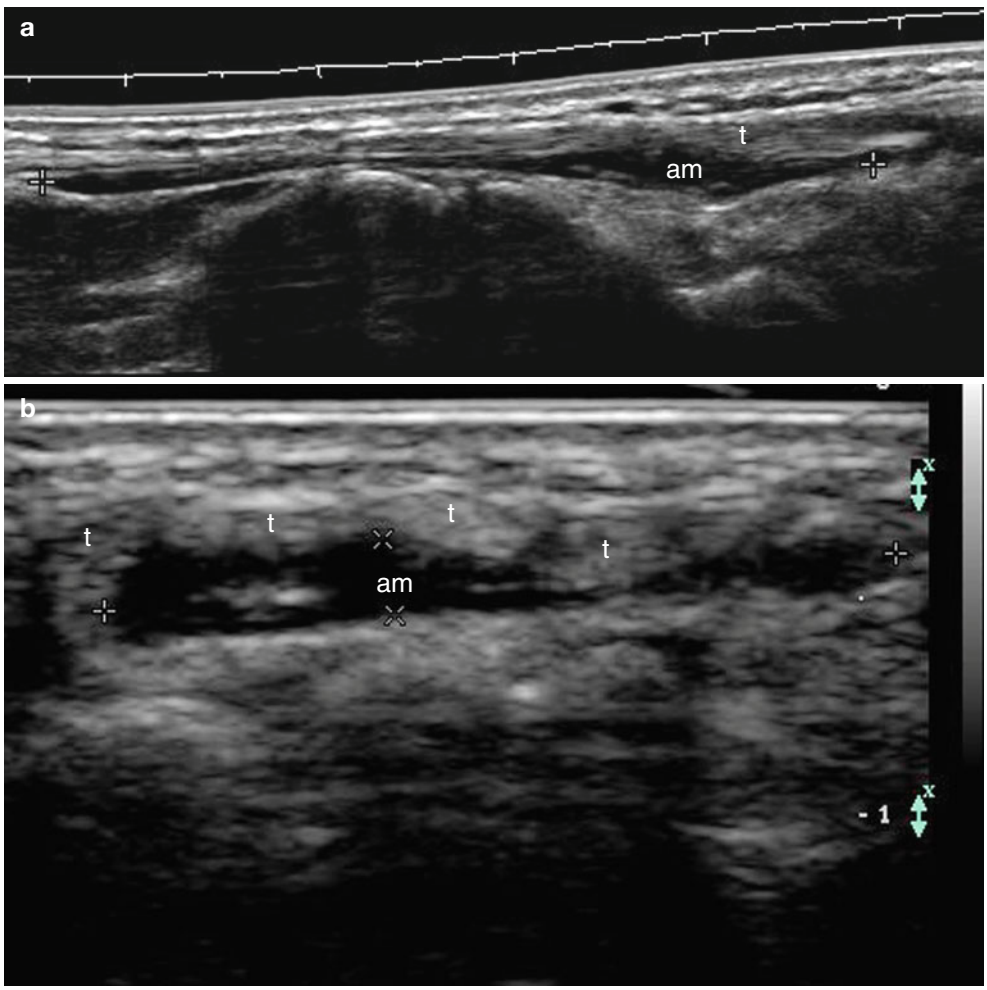

Fig. 2.14 (**a**, **b**) Accessory muscle. (**a**) Ultrasound of the dorsum of the wrist and hand (longitudinal panoramic view). The hypoechoic structure (*am*) attached to the common extensor tendons (*t*) corresponds to an accessory muscle (extensor digitorum brevis manus). (**b**) Ultrasound of the same dorsum of the wrist and hand in transverse view)

Table 2.1 Common limb accessory muscles

Muscle	Location
Chondroepitrocleariis	Arm
Anconeous	Elbow
Anoumalous palmaris longus	Forearm
Lumbrical muscles (proximal origin)	Wrist and hand
Flexor digitorum superficialis of the index finger	Wrist and hand
Abductor digiti minimi	Wrist and hand
Extensor digitorum brevis	Wrist and hand
Tensor fasciae surale	Knee
Accessory soleus	Ankle
Peroneous quartus	Ankle
Accessory flexor digitorum longus	Ankle

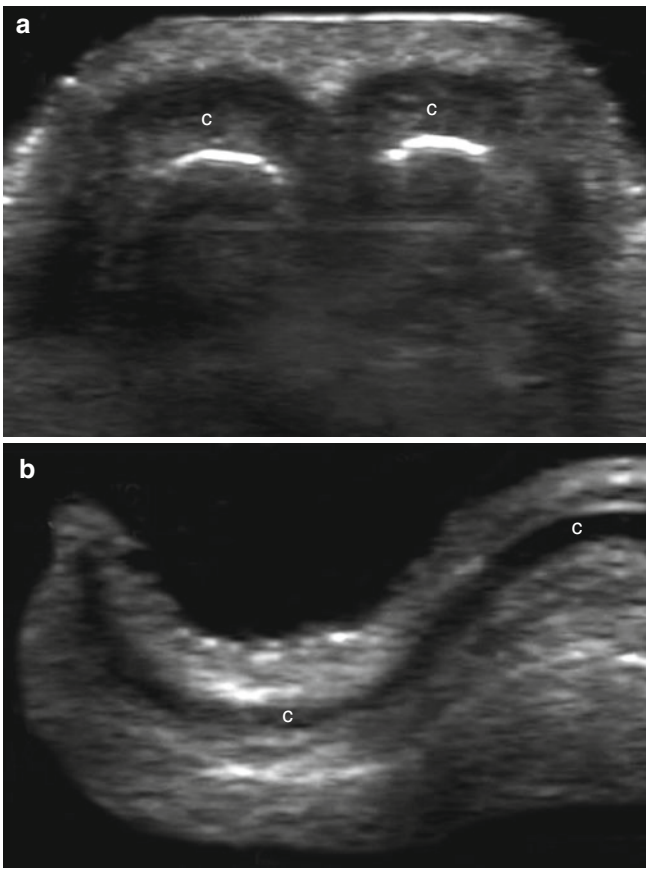

Fig. 2.15 (**a**, **b**) Anatomy of cartilage. (**a**) Ultrasound at the tip of the nose (transverse view). Note hypoechoic nasal cartilages (*c*). (**b**) Ultrasound at the middle third of the ear pinna (transverse view). Note hypoechoic sinuous band of the auricular cartilage (*c*)

shoulder and the gastrocnemius-semimembranous bursae in the knee. They may (for e.g., suprapatellar bursa) or may not (for e.g., infrapatellar bursa) communicate with the joint; bursae may even develop de novo, in response to friction or pressure over bony prominences as in hallux valgus, or exostoses. Under pathological conditions, bursae can undergo marked swelling and become large fluid-filled

Table 2.2 Subcutaneous bursae location

Bursa	Anatomic location
Olecranon	Posterior elbow
Baastrup	Spinous processes
Throcanteric	Hip
Prepatellar	Anterior knee
Infrapatellar	Anterior knee
Tibial tuberosity	Anterior knee
Calcaneal	Posterior ankle (Achilles tendon)

structures (bursitis); common locations of subcutaneous bursitis are shown in Table 2.2 [22].

2.5.5.2 Sonography

Inflamed bursae are commonly detectable using sonography and appearing as anechoic fluid-filled sac-like structures, sometimes surrounded by thick hypoechoic borders. In cases of mild inflammation, a hypoechoic band can be the only sonographic finding (Fig. 2.16).

2.5.6 Blood Vessels

2.5.6.1 Anatomy

Blood vessels are vascular channels that are part of the circulatory system and are separated in arteries, veins, and a capillary endothelial network. In contrast to veins, arteries present a smooth muscle layer, and the course of major blood vessels is well described in the literature. Clinical assessment involves palpation, however, a number of vascular diseases and abnormalities can be described more accurately using sonography.

2.5.6.2 Sonography

Blood vessels are characterized sonographically by their typical tubular shape and anechoic structure; veins usually collapse the lumen when compressed with the probe, while arteries do not collapse to compression. Atheromatosis may produce hypoechoic intimal thickening and, if calcified, may change to hyperechoic sometimes with posterior acoustic shadowing artifact. Phleboliths are calcifications that appear as hyperechoic deposits usually within the veins lumen. Color Doppler spectral curve analysis can readily distinguish arteries from veins; arterial vessels generally show systolic and diastolic peaks, while venous vessels exhibit monophasic tracings (Fig. 2.17).

2.5.6.3 Variant: Caliber Persistent Arteries (CPA)

CPAs are developmental alterations where arterial vessels fail to undergo the normal loss in caliber after penetrating the submucosal space. These anomalous arteries, often found in the lower lip as asymptomatic papules, can be misdiagnosed as malignant skin tumors, or can cause unexpected bleeding

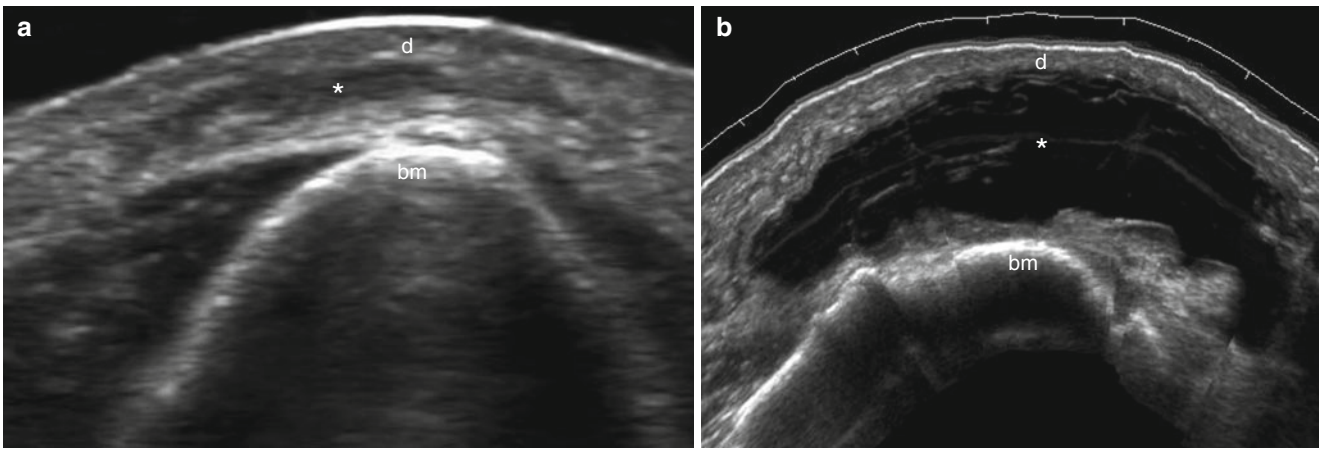

Fig. 2.16 (**a**, **b**) Anatomy of bursae. (**a**) Ultrasound at the tip of the olecranon (transverse view). Note slight hypoechoic thickening of olecranon bursa capsule (*). (**b**) Ultrasound at the posterior elbow (transverse panoramic view). The olecranon bursa is moderately enlarged with anechoic fluid (*). Abbreviations: *d* dermis, *bm* bony margin of the olecranon

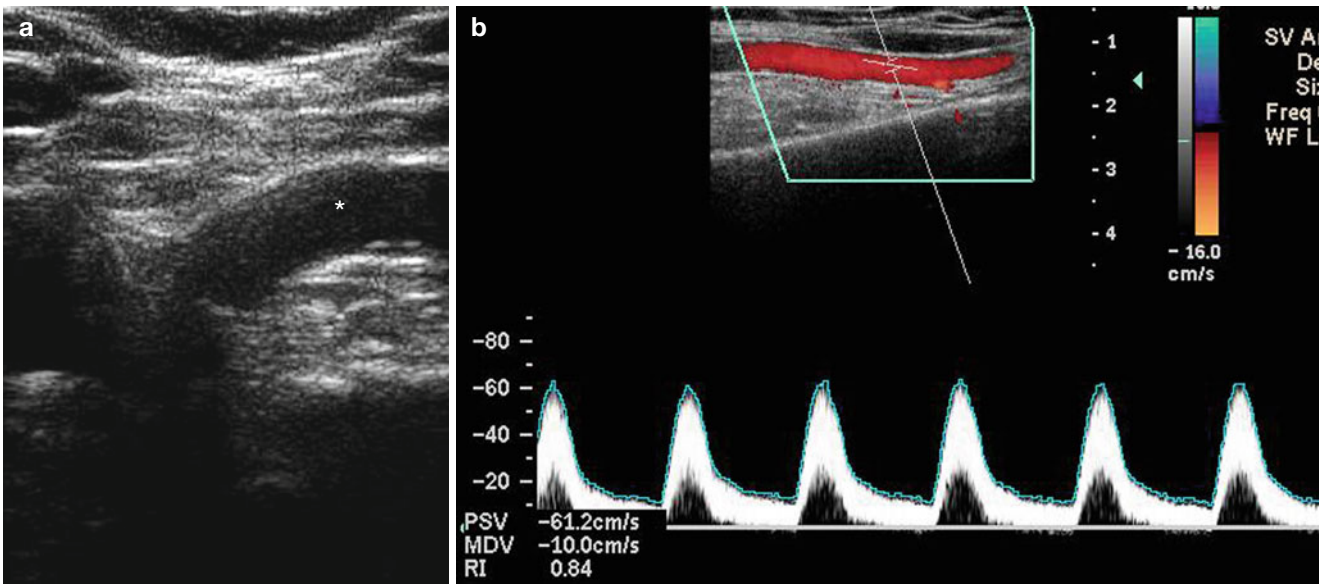

Fig. 2.17 (**a**, **b**) Anatomy of blood vessels. (**a**) Ultrasound at the supraclavicular region (transverse view). The tubular anechoic structure corresponds to the subclavian artery. (**b**) Color Doppler ultrasound with spectral curve analysis of blood flow at the axillary artery; plot of peak systolic velocity is depicted at the bottom

during biopsy or surgical procedures [23, 24]. On sonography, CPA appear as anechoic and often tortuous tubular structures of persistent caliber after entering the dermis of the lips. Color Doppler ultrasound demonstrates arterial pattern of flow within the anomalous vessel (Fig. 2.18).

2.5.7 Nerves

2.5.7.1 Anatomy

Peripheral nerves are made of axons held together by a thin endoneurium (inner layer), grouped into fascicles covered by the perineurium, and gathered into the nerve that is surrounded by the epineurium (outer layer). Nerves can be directly involved in disease, but imaging may also be used in connection with regional nerve blocks.

2.5.7.2 Sonography

Sonography shows nerves as hypoechoic structures with fine fascicular pattern; nerves on the traverse axis may resemble the sonographic appearance of the ovary in shape and echogenicity because they contain numerous hypoechoic dots corresponding to the fascicular disposition (Fig. 2.19). Nerves usually run close to vascular structures, and they are susceptible to suffering entrapment syndromes in selected anatomical locations that commonly involve fibro-osseous

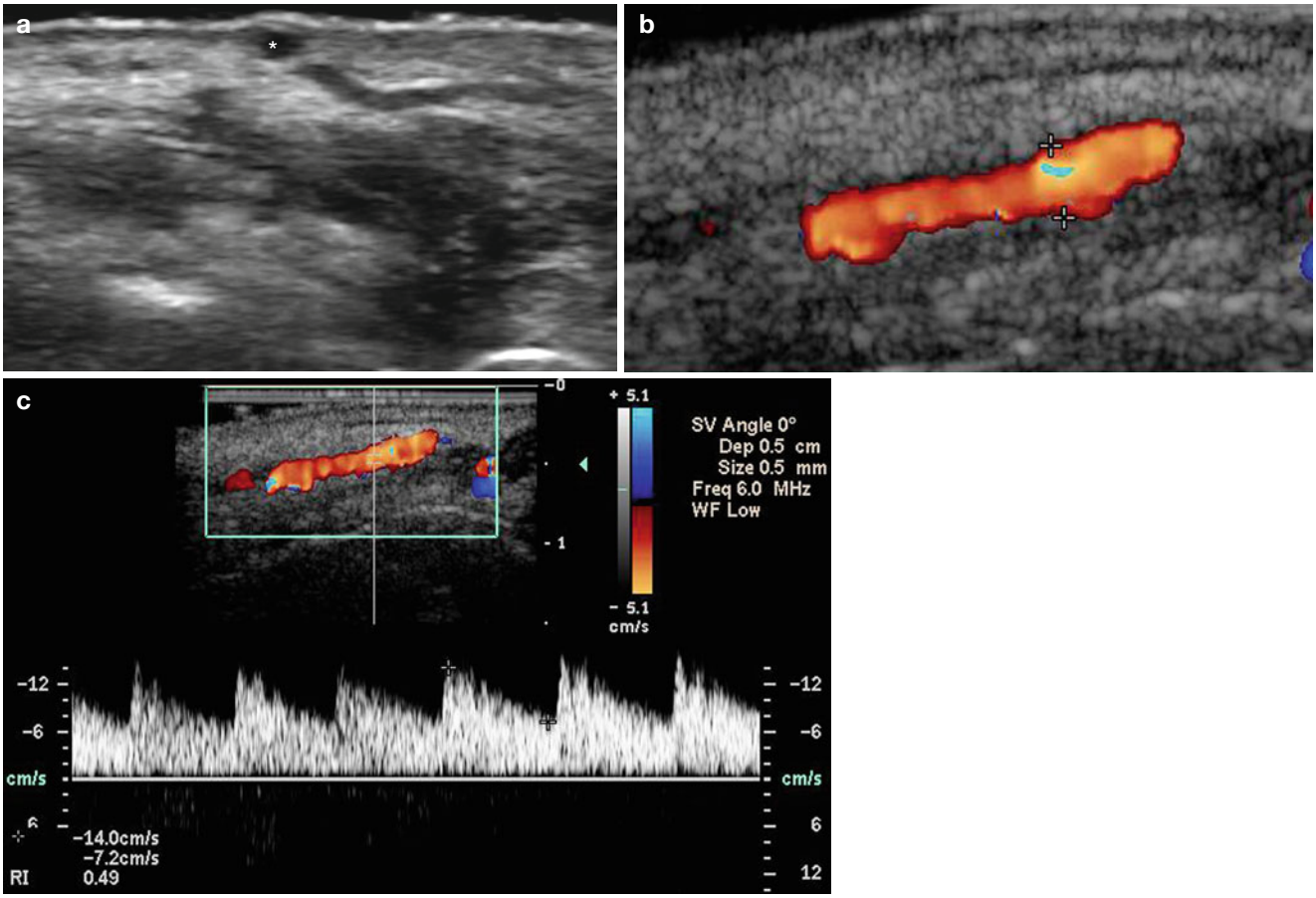

Fig. 2.18 (**a**–**c**) Caliber persistent artery of the lip. (**a**) Ultrasound (gray scale, transverse view) shows an anechoic round shaped nodule (*) in the dermis close to a tubular anechoic tract. (**b**) Color Doppler ultrasound (oblique view) demonstrates flow within the superficial tubular structure that was connected to the anechoic nodule and running superficially located to the orbicularis oris muscle. (**c**) Color Doppler ultrasound spectral curve analysis (oblique view) shows arterial blood flow within the vessel

tunnels such as the carpal or cubital tunnel in the wrist and elbow, respectively.

2.5.7.3 Variant: Bifid Median Nerve and Persistent Median Artery

Occasionally, nerves that normally present as single structures may instead present as two separate branches, a condition called bifid nerve that nevertheless shows similar fascicular echo-structures as single nerves. A common substrate for this anatomic variant is the median nerve that becomes bifid at the wrist, usually associated with a persistent median artery running between the branches; it is present in 15.4 % of healthy individuals and conversely, up to 63 % of the cases of persistent median artery are associated with a bifid median nerve. A unilateral persistent median artery is present in 20 % of normal subjects, and the bilateral form in 6 % of the general population. While the persistent median artery is most commonly seen as a hypoechoic thin fibrous remnant, it occasionally may show blood flow on color Doppler and rarely, vessel widening or even a hypoechoic thrombus within the lumen. Because of its superficial course close to the transverse carpal ligament, it has the potential for being injured during unrelated surgery and a preoperative diagnosis of persistent median artery can be clinically helpful [25–28] (Fig. 2.20).

2.5.8 Salivary Glands

2.5.8.1 Anatomy

Salivary glands are exocrine glands in charge of the secretion of saliva. They are located in proximity to the face and are easily detectable during sonographic examinations. They can be separated into major (parotid and submandibular) and minor salivary glands (oral cavity or lips region)

2.5.8.2 Sonography

The parotid glands are seen in their pre-auricular location in healthy individuals, with a characteristic sonographic hyperechoic parenchyma sometimes containing lymph nodes. Both submandibular glands appear as oval-shaped

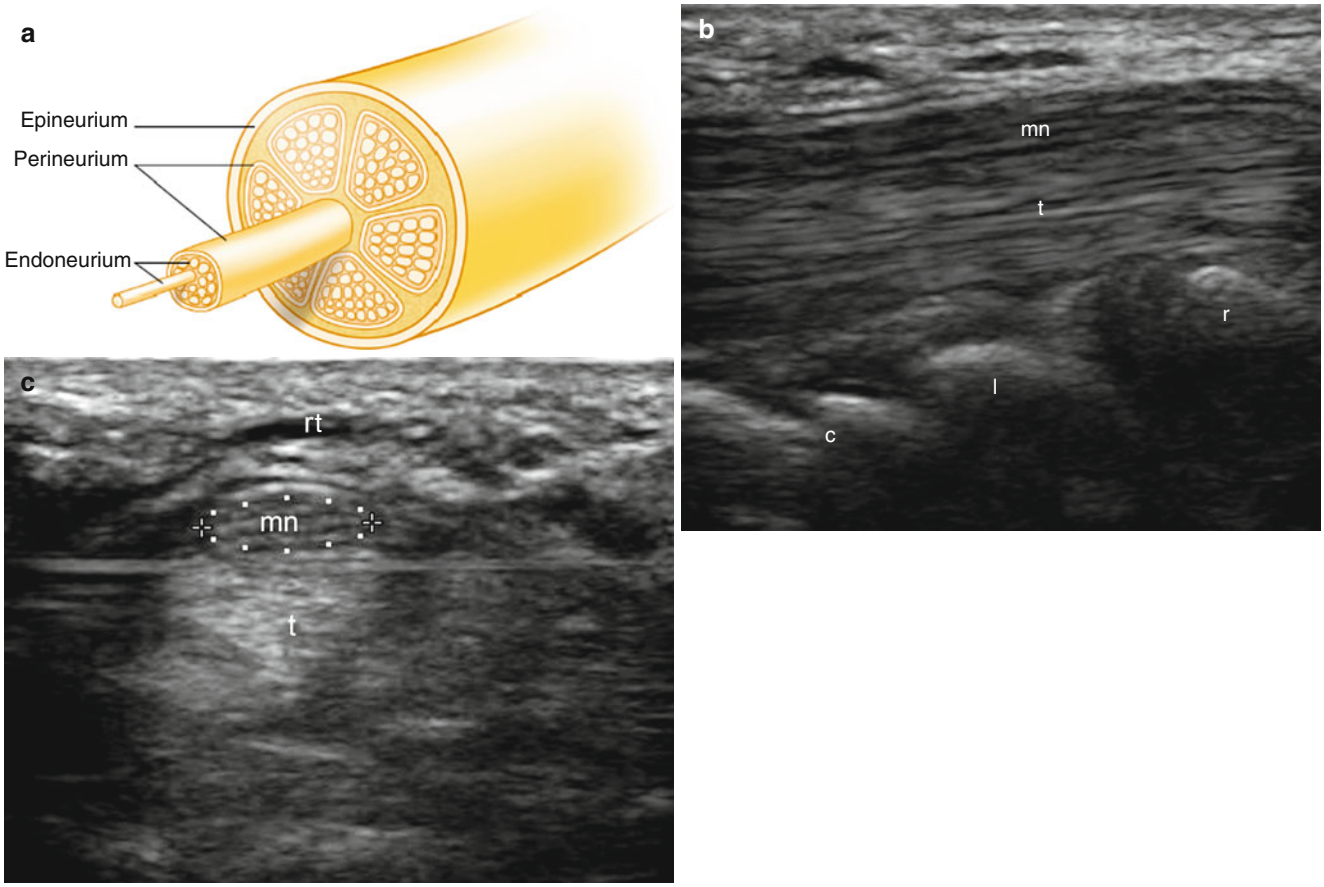

Fig. 2.19 (**a**–**c**) Normal anatomy of the nerve. (**a**) Schematic representation of a nerve. (**b**) Ultrasound of the median nerve at the wrist (longitudinal view). The hypoechoic pattern of the nerve allows easy separation from the hyperechoic tendons (*t*). (**c**) Ultrasound of the median nerve (transverse view) showing characteristic fascicular pattern with hypoechoic dots. *Abbreviations*: *mn* median nerve, *t* flexor tendons, *r* radius, *l* lunate, *c* capitate, *rt* flexor retinaculum

structures, either hyperechoic or slightly hypoechoic. Minor salivary glands appear as round-shaped hypoechoic structures (Fig. 2.21). On color Doppler low-velocity blood flow can be detected in the major glands.

2.5.8.3 Variant: Accessory or Anomalous Salivary Glands

Accessory or anomalous salivary glands are located in an ectopic location and with a well-formed ductal system; in contrast, heterotopic glands that are also in an abnormal location exhibit only rudimentary salivary tissue that consists solely of glandular acini. Accessory parotid glands are common, unilateral or bilateral, usually being found in the cheek, between the main parotid gland and the masseter fascia, immediately above the parotid duct, into where it drains through a tributary duct, and is found at autopsy in 21–56 % of normal adults. The differential diagnosis of the anomalous gland must include an anterior extension or "facial process" of the parotid gland fully connected to the main gland. Accessory parotid glands can occasionally produce facial swelling or asymmetry; they may become a source of complications during cosmetic facial procedures, or become affected by salivary glands tumors (up to 8 % of parotid tumors occur from accessory glands). If considering only malignant salivary gland tumors, the second most common location is the accessory salivary glands with a frequency of 22.6 %, immediately after the parotid glands with a relative frequency of 57.5 % [29–31]. On sonography, accessory glands show similar echostructure but smaller size than the main glands (Fig. 2.22).

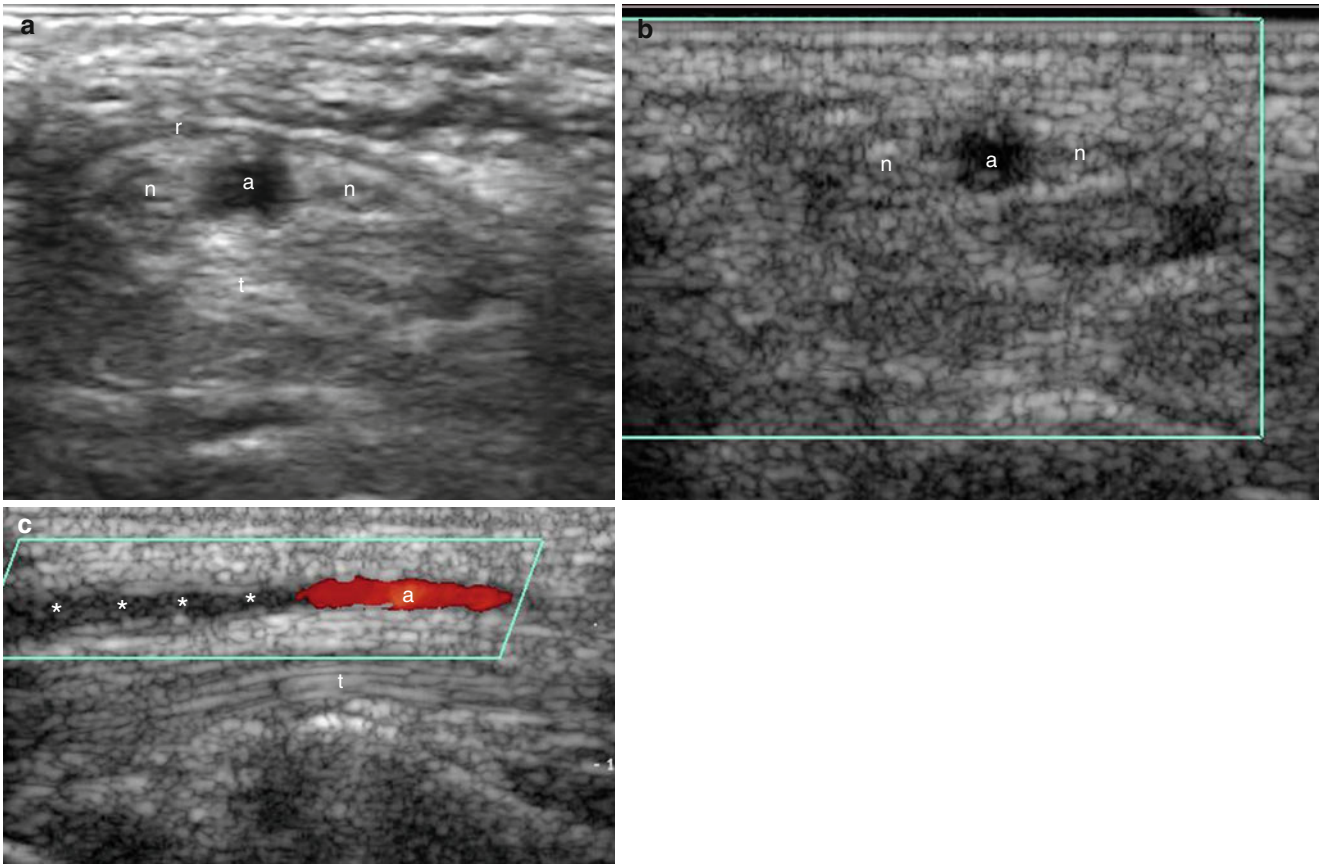

Fig. 2.20 (**a**, **b**) Bifid median nerve and persistent median artery. (**a**) Ultrasound of the wrist (transverse view). Two branches of the median nerve (*n*) are separated by a dilated persistent median artery (*a*). (**b**) Color Doppler ultrasound (longitudinal view) showing the vessel lumen to be partially hypoechoic indicaticating arterial thrombosis (*), with corresponding lack of blood flow signals. The proximal artery segment shows colorful blood flow. *Abbreviations*: *a* persistent median artery, *t* flexor tendons, *r* flexor retinaculum

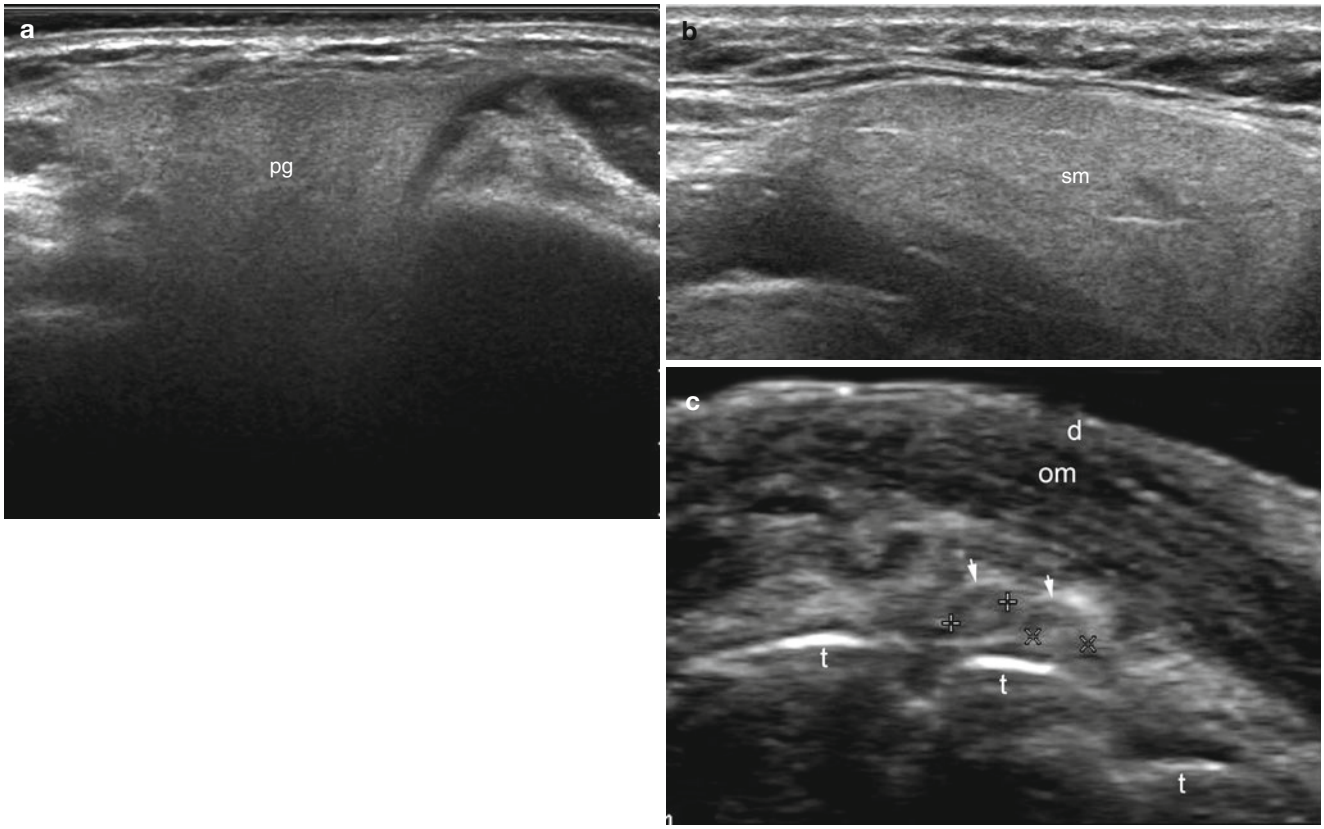

Fig. 2.21 (**a**–**c**) Anatomy of the salivary glands. (**a**) Ultrasound of the parotid gland (transverse view). Note hyperechoic homogenous pattern. (**b**) Ultrasound of the submandibular gland (transverse view) shows homogenous echogenicity and oval shape. (**c**) Ultrasound of the upper lip (transverse view). Minor salivary glands appear as hypoechoic round-shaped structures (*arrows* and between markers). *Abbreviations*: *d* dermis, *om* orbicularis oris muscle, *t* tooth, *pg* parotid gland, *sm* submandibular gland

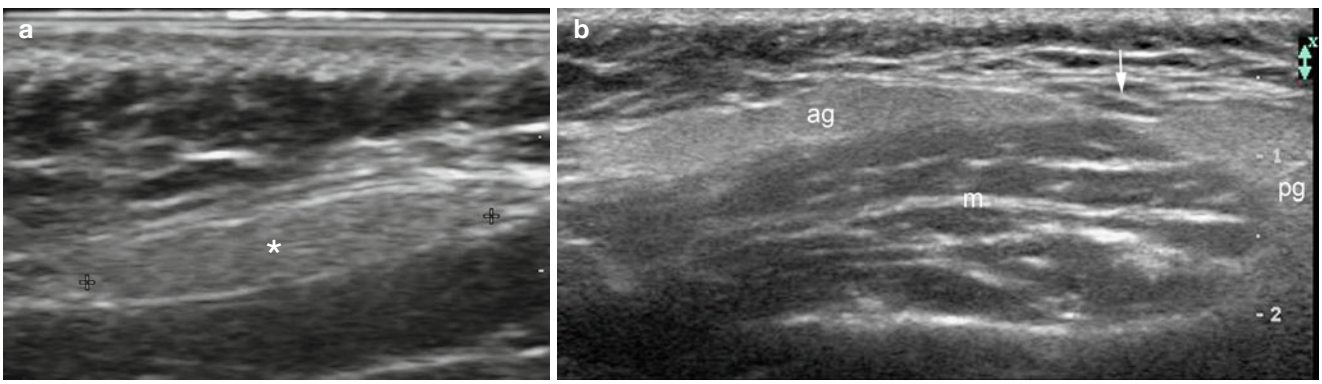

Fig. 2.22 (**a**, **b**) Accessory salivary glands. (**a**) Ultrasound (transverse view) at the right cheek shows hyperechoic oval-shaped and well-defined structure (*, between markers) adjacent to the surface of the masseter muscle. (**b**) Ultrasound in another case (transverse and wider view, left cheek). The accessory salivary gland is close to the masseter muscle, but separated from the parotid gland (*pg*). The separation is marked with an *arrow*

References

1. Proksch E, Brandner JM, Jensen JM. The skin: an indispensable barrier. Exp Dermatol. 2008;17:1063–72.
2. McKee P, Calonje E, Granter S. The structure and function of skin. In: McKee P, Calonje E, Granter S, editors. Pathology of the skin with clinical correlations. Philadelphia: Elsevier/Mosby; 2005. p. 1–36.
3. Ebling FJG, Eady RAJ, Leigh IM. Anatomy and organization of human skin. In: Rook AJ, Wilkinson DS, Ebling FJG, editors. Textbook of dermatology. Oxford: Blackwell Scientific Publications; 1992. p. 49.
4. Wortsman X, Wortsman J. Clinical usefulness of variable frequency ultrasound in localized lesions of the skin. J Am Acad Dermatol. 2010;62:247–56.
5. Farinelli N, Berardesca E. The skin integument: variation relative to sex, age, race, and body region. In: Serup J, Jemec GBE, Grove GL, editors. Handbook of non-invasive methods and the skin. 2nd ed. Boca Raton: Taylor and Francis; 2006. p. 27–31.
6. Wortsman XC, Holm EA, Wulf HC, Jemec GB. Real-time spatial compound ultrasound imaging of skin. Skin Res Technol. 2004; 10:23–31.
7. Kanitakis J. Anatomy, histology and immunohistochemistry of normal human skin. Eur J Dermatol. 2002;12:390–9.
8. Burns DA, Breathnach SM, Cox N, Griffiths CE, editors. Rook's textbook of dermatology. 7th ed. Malden: Blackwell Science; 2004. p. 3.1–3.84.
9. Gniadecka M, Gniadecki R, Serup J, Søndergaard J. Ultrasound structure and digital image analysis of the subepidermal low echogenic band in aged human skin: diurnal changes and interindividual variability. J Invest Dermatol. 1994;102:362–5.
10. Ackerman AB. Panniculitis. In: Ackerman AB, editor. Histopathologic diagnosis of inflammatory skin diseases. Philadelphia: Lea & Febiger; 1978. p. 779–825.
11. Segura S, Requena L. Anatomy and histology of normal subcutaneous fat, necrosis of adipocytes, and classification of the panniculitides. Dermatol Clin. 2008;26:419–24.
12. Requena L. Normal subcutaneous fat, necrosis of adipocytes and classification of the panniculitides. Semin Cutan Med Surg. 2007;26:66–70.
13. de Berker D, Baran R. Science of the nail apparatus. In: Baran R, de Berker D, Holzberg M, Thomas L, editors. Baran & Dawber diseases of the nails and their management. 4th ed. Oxford: Wiley-Blackwell; 2012. p. 1–50.
14. Wortsman X, Wortsman J, Soto R, Saavedra T, Honeyman J, Sazunic I, et al. Benign tumors and pseudotumors of the nail: a novel application of sonography. J Ultrasound Med. 2010;29: 803–16.
15. Amirlak B, Shahabi L, Campbell AC, Totonchi A, Soltanian H. Skin anatomy. Medscape. http://emedicine.medscape.com/article/1294744-overview#showall
16. Schneider MR, Schmidt-Ullrich R, Paus R. The hair follicle as a dynamic miniorgan. Curr Biol. 2009;19:R132–42.
17. Wortsman X, Wortsman J, Matsuoka L, Saavedra T, Mardones F, Saavedra D, et al. Sonography in pathologies of scalp and hair. Br J Radiol. 2012;85:647–55.
18. Van Holsbeeck M, Introcaso J. Sonography of tendons. In: Van Holsbeeck M, Introcaso J, editors. Musculoskeletal ultrasound. 2nd ed. St. Louis: Mosby; 2001. p. 77–129.
19. Van Holsbeeck M, Introcaso J. Sonography of muscle. In: Van Holsbeeck M, Introcaso J, editors. Musculoskeletal ultrasound. 2nd ed. St. Louis: Mosby; 2001. p. 23–75.
20. Wortsman X, Azocar P. Wrist ultrasound. In: Dogra V, Gaitini D, editors. Musculoskeletal ultrasound with CT and MRI correlation. 1st ed. New York/Stuttgart: Thieme; 2010. p. 46–70.
21. Wortsman X, Jemec GB. Sonography of the ear pinna. J Ultrasound Med. 2008;27:761–70.
22. Van Holsbeeck M, Introcaso J. Sonography of bursae. In: Van Holsbeeck M, Introcaso J, editors. Musculoskeletal ultrasound. 2nd ed. St. Louis: Mosby; 2001. p. 131–69.
23. Wortsman X, Calderón P, Arellano J, Orellana Y. High-resolution color Doppler ultrasound of a caliber-persistent artery of the lip, a simulator variant of dermatologic disease: case report and sonographic findings. Int J Dermatol. 2009;48:830–3.
24. Arellano J, Antoniazzi C, Wortsman X. Early diagnosis of a calibre persistent labial artery in a child: usefulness of ultrasonography. Australas J Dermatol. 2012;53:e18–9.
25. Granata G, Caliandro P, Pazzaglia C, Minciotti I, Russo G, Martinoli C, et al. Prevalence of bifid median nerve at wrist assessed through ultrasound. Neurol Sci. 2011;32:615–8.
26. Gassner EM, Schocke M, Peer S, Schwabegger A, Jaschke W, Bodner G. Persistent median artery in the carpal tunnel: color Doppler ultrasonographic findings. J Ultrasound Med. 2002;21:455–61.
27. Propeck T, Quinn TJ, Jacobson JA, Paulino AF, Habra G, Darian VB. Sonography and MR imaging of bifid median nerve with anatomic and histologic correlation. AJR Am J Roentgenol. 2000; 175:1721–5.
28. Iannicelli E, Chianta GA, Salvini V, Almberger M, Monacelli G, Passariello R. Evaluation of bifid median nerve with sonography and MR imaging. J Ultrasound Med. 2000;19:481–5.
29. Ostman J, Anneroth G, Gustafsson H, Tavelin B. Malignant salivary gland tumours in Sweden 1960–1989 – an epidemiological study. Oral Oncol. 1997;33:169–76.
30. Ito FA, Ito K, Vargas PA, de Almeida OP, Lopes MA. Salivary gland tumors in a Brazilian population: a retrospective study of 496 cases. Int J Oral Maxillofac Surg. 2005;34:533–6.
31. Cunnane M, Artz G. Histology epithelial metaplasias and non inflammatory and non neoplastic lesions of the salivary glands. In: Lee Witt R, editor. Salivary glands diseases: surgical and medical management. New York: Thieme; 2006. p. 50.